Technische Universität München

Fakultät für Medizin

Klinik und Poliklinik für RadioOnkologie und Strahlentherapie
Klinikum rechts der Isar

ALDH1A1 knockdown increases radiosensitivity and reduces migration in glioblastoma cells

Friederike Martin

Vollständiger Abdruck der von der Fakultät für Medizin der Technischen Universität München zur Erlangung des akademischen Grades eines Doktors der Medizin genehmigten Dissertation.

Vorsitzender:	Prof. Dr. Jürgen Schlegel
Prüfende der Dissertation:	1. Prof. Dr. Stephanie E. Combs 2. Priv.-Doz. Dr. Friederike Schmidt-Graf

Diese Dissertation wurde am 07.03.2019 bei der Technischen Universität München eingereicht und durch die Fakultät für Medizin am 08.10.2019 angenommen.

28.3.2013 9:40

Eine Prognose gibt es nicht, eine allgemeine Statistik auch nicht mehr. Nach drei OPs, zwei Bestrahlungen, drei verschiedenen Chemos ist man seine eigene Statistik.

Vor drei Jahren noch war ich ein winziger Punkt in einer Punktwolke, reine Mathematik, kein Individuum, das hatte mir gefallen. Jetzt weiß ich nicht mehr. Keiner weiß.

Aus „Arbeit und Struktur“ von Wolfgang Herrndorf -
Herrndorf nahm sich 3 Jahre nach der Erstdiagnose eines Glioblastoms im Dezember 2013 das Leben.

Contents

Abbreviations III

1 Introduction 1

1.1 Glioblastoma multiforme 1

1.1.1 Epidemiology 1

1.1.2 Etiology 1

1.1.3 Pathology and classification 1

1.1.4 Tumorigenesis 4

1.1.5 Clinical presentation 5

1.1.6 Treatment and therapy resistance 6

1.2 ALDH1A1 9

1.2.1 ALDH superfamily 9

1.2.2 ALDH1A1 10

2 Objectives 12

3 Methods and Materials 13

3.1 Materials 13

3.1.1 Cell line 13

3.1.2 Technical devices 13

3.1.3 Software 14

3.1.4 Chemicals and reagents 14

3.1.5 Consumables 17

3.2 Methods 18

3.2.1 Cell culture 18

3.2.2 ALDH1A1 knockdown with shRNA 19

3.2.3 Western blot analysis 21

3.2.4 Clonogenic assay 24

3.2.5 Migration assay / Wound healing assay 25

3.2.6 Proliferation assay 26

3.2.7 Analysis of cell cycle distribution 27

3.2.8 Irradiation 27

3.2.9 Hypoxia 28

3.2.10 Statistics 28

4 Results 29

4.1 Generation of stable ALDH1A1 knockdown in GBM cell line LN18 29

4.2 ALDH1A1 knockdown has no influence on proliferation but plating efficiency 32

4.3 ALDH1A1 knockdown leads to enhanced radiosensitivity 33
4.4 ALDH1A1 knockdown has no influence on cell cycle distribution after irradiation 35
4.5 ALDH1A1 knockdown decreases migratory capacity in LN18 GBM cells 38
4.6 X-ray irradiation does not affect migration of ALDH1A1+ and ALDH1A1- LN18 GBM cells 41
4.7 Hypoxia has no influence on ALDH1A1 expression 43

5 Discussion 44

5.1 Stable ALDH1A1 knockdown in GBM cells – a proper model to investigate the function of ALDH1A1 in GBM? 44
5.2 ALDH1A1 expression and GBM cell proliferation 45
5.3 ALDH1A1 expression and radioresistance in GBM cells 46
5.4 The impact of ALDH1A1 expression on migration of GBM cells 48
5.4.1 Influence of irradiation on migration in GBM 49
5.5 Evaluation of the influence of hypoxia on ALDH1A1 expression 50
5.6 ALDH1A1 as a new prognostic marker and therapy target in GBM 50

6 Summary and Outlook 52

7 Danksagung 53

Figures V

Tables VIII

References IX

Abbreviations

4-HNE	4-Hydroxynonenal
ALDH	Aldehyde dehydrogenase
ALDH1A1-	LN18 cells with ALDH1A1 knockdown
ALDH1A1+	LN18 control cells without ALDH1A1 knockdown
CA 9	Carbonic anhydrase IX
CDK	Cyclin-dependent-kinase
CSC	Cancer stem cell
CT	Computed tomography
DDR	DNA damage repair
DEAB	Diethylaminobenzaldehyde
DFS	Disease free survival
DNA	Deoxyribonucleic acid
DT	Doubling Time
EGFR	Epidermal growth factor receptor
EMT	Epithelial to mesenchymal transition
EORCT	European Organisation for Research and Treatment of Cancer Cancer
FACS	Fluorescence-activated cell sorting
GBM	Glioblastoma multiforme
GCSC	Glioblastoma cancer stem cell
Gy	Gray
HIF	Hypoxia inducible factor
IDH	Isocitrate dehydrogenase
LOH	Loss of heterozygistiy
MDA	3,4-Methylenedioxyamphetamin
MGMT	O^6-methylguanin-DNA-transferase
MMP	Matrix metalloproteinase
MRI	Magnetic resonance imaging
MST	Mean survival time
NAD	Nicotinamide adenine dinucleotide
NADP	Nicotinamide adenine dinucleotide phosphate
NCIC	National Cancer Institute of Canada Clinical Trials Group
NF 1	Neurofibromatosis type 1
OS	Overall survival
PDGFRA	Platelet-derived growth factor receptor alpha
PE	Plating efficiency
PTEN	Phosphatase and tensin homolog
RADH 1	Retinaldehyde dehydrogenase 1
ROS	Reactive oxygen species
SD	Standard deviation
SEM	Standard error of the mean
SER	Sensitizing enhancement ratio
SHH	Sonic hedgehog

shRNA	Short hairpin ribonucleic acid
SOX-2	Sex determing region Y – box 2
TMZ	Temozolomide
TP53	Tumor protein 53
VEGF	Vascular endothelial growth factor
WHO	World health organisation
Wnt	Wingless/Integrated

1 Introduction

1.1 Glioblastoma multiforme

1.1.1 Epidemiology

Glioblastoma multiforme (GBM), a WHO grade IV tumor, is the most common primary brain tumor in adults. The incidence rate of glioblastoma in the United States is 3.9 per 100000 and is slightly higher in males than in females (1.6:1). Precise data for incidence rate of GBM specific for Germany are not available because most of the studies show combined data for all central nervous system tumors or at least more specific for all astrocytic tumors. Median survival of GBM patients under 70 years is still very short with 15 months after first diagnosis and best available treatment. For patients older than 70 years it´s even worse (Lawrence et al. 2012). Recurrence of the tumor after primary treatment seems to be inevitable. 5-years-survival is around 10 % for primary and 3 % for secondary GBM (IARC (International Agency for Research on Cancer) 2014). No recent numbers exist about GBM relapses, because a uniform definition of GBM recurrence is still missing (Hou et al. 2006).

1.1.2 Etiology

The etiology of GBM is still unknown. Several risk factors which may lead to the development of GBM are discussed. Some rare genetic disorders are associated with increased incidence of GBM. These are Neurofibromatosis 1 and 2, Tuberous sclerosis, Retinoblastoma, Li-Fraumeni syndrome, Turcot´s syndrome and multiple hamartoma (Schwartzbaum et al. 2006). Except for these inherited mutations, the only verified exogenous risk factor for GBM is exposure to therapeutic ionizing radiation, especially in childhood (Ostrom et al. 2014, Rees et al. 2016).

1.1.3 Pathology and classification

GBMs are characterized by heterogeneous cell populations (cells with astrocytic or oligodendroglial features or mixed cellular features), high invasiveness and infiltration, neovascularization and by the occurrence of necrotic areas within the tumor. The necrotic areas are surrounded by so-called pseudopallisadic cells and hypoxic regions (Maher et al. 2001, Furnari et al. 2007, Zong et al. 2012).

Two different types of GBM are described. Primary GBMs which make up 95% of all GBMs and secondary GBMs which make up 5% of all GBMs (Ohgaki et al. 2004). Primary and secondary GBMs differ in their genesis and therefore in their genomic alterations and clinical presentation. Primary GBMs occur de novo mainly in older patients and develop rapidly. Secondary GBMs progress from low-grade diffuse astrocytomas or anaplastic astrocytomas and occur mostly in younger patients (Ohgaki and Kleihues 2005, Ohgaki and Kleihues 2013). Distinct genomic alterations of primary and secondary GBM are shown in Figure 1.1.

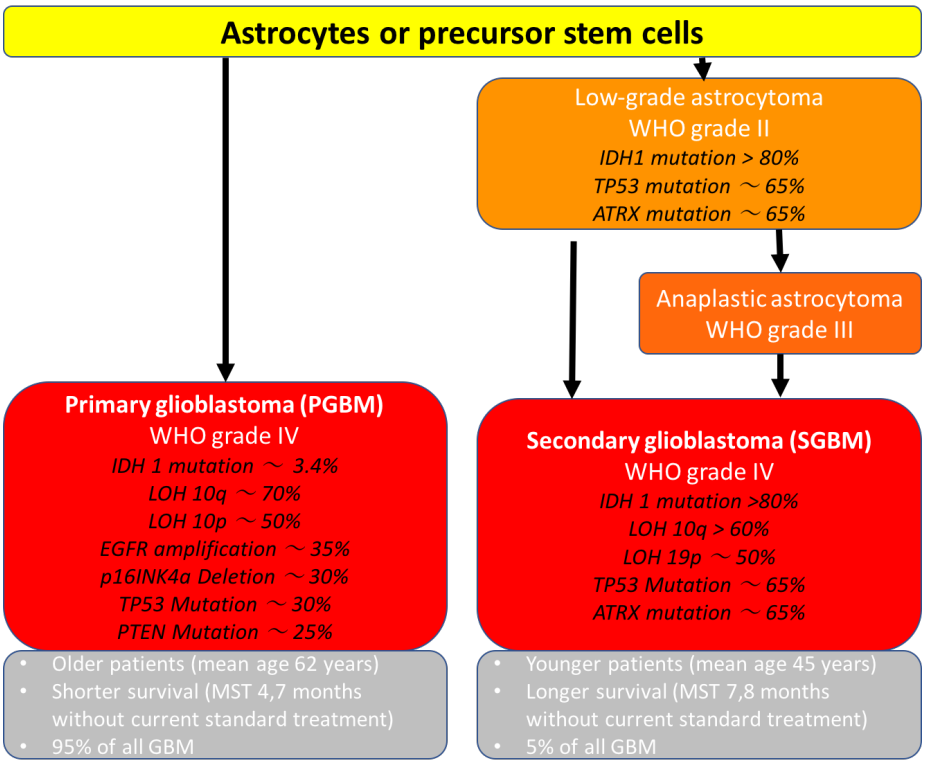

Figure 1.1 Genetic pathways to primary and secondary GBM and their clinical differences modified from (Ohgaki et al. 2004, Ohgaki and Kleihues 2013). (EGFR, epithelial growth factor receptor; IDH1, isocitrate dehydrogenase 1; LOH, loss of heterozygosity; p16ink4a, cyclin-dependent kinase inhibitor 2A; PTEN, phosphatase and tensin homolog; TP53, tumor protein p53; MST, mean survival time).

Besides this GBMs can be classified in four subtypes, defined by the TCGA (The Cancer Genome Atlas) which characterizes GBMs by their gene expression patterns, their different clinical characteristics and their response to therapy (see Table 1.1). The classification of different GBM subtypes is supposed to be important for the optimal therapeutic decision-making and could serve as a prognostic factor (Verhaak et al. 2010). Different subtypes of GBM may coexist in the same tumor or patient (Sottoriva et al. 2013).

Table 1.1 GBM subtypes: Genetic and clinical characteristics (Verhaak et al. 2010)

Subtype	***Genomic abnormalities***	***Remark***
Classical	• Chromosome 7 amplification paired with loss of chromosome 10 • High level EGFR amplification and increased EGFR expression • Focal 9p21.3 homozygous deletion, targeting CDKN2A • High expression of NES, Notch and Sonic hedgehog signaling pathways • Lack of TP53 mutations	• Good response to aggressive therapy • Most common type of GBM

Proneural	• Mutations in IDH1 • High expression of PDGFRA • Mutations in TP53 • LOH 10 • High expression of oligodendrocytic development genes	• No response to aggressive therapy • Younger age
Mesenchymal	• Mutations in NF 1, PTEN and TP53 • Higher expression of mesenchymal and astrocytic markers such as CD44 and MERTK • High expression of genes in the tumor necrosis factor family pathway and the NF-κB pathway	• Good response to aggressive therapy • Higher percentage of inflammation and necrosis
Neural	• Expression pattern most similar compared to normal brain tissue	

1.1.3.1 Migration of GBM cells

The invasion into surrounding tissue due to the migratory capability of GBM cells is a key part of the high malignancy of this tumor entity. Migration and invasion might enable tumor cells to escape radical surgery, radiotherapy and maybe chemotherapy. Hence, GBM cells with migratory capacity might be responsible for tumor relapse.

Unlike most other solid tumors, GBM rarely metastasize outside the brain (Lun et al. 2011). Instead of intravascular or lymphatic metastatic spread, GBM cells migrate along the so-called Scherer´s secondary structures, namely: the perivascular space, the brain parenchyma, white matter tracts and the subarachnoid space (Cuddapah et al. 2014).

However, not all cells within the GBM tumor bulk are capable to migrate. Recent research tried to identify the migrating cell subpopulation in GBM tumors. Munthe et al. (2016) could show, that migrating GBM cells display cancer stem cell (CSC) characteristics, such as the expression of the cell surface markers CD44 and SOX-2. The study could also show, that GBM cells with migratory capability could initiate tumor regrowth (Munthe et al. 2016). This again hints to the idea, that GBM cells with the ability to migrate could be responsible for tumor relapse.

One possible trigger for GBM cells to acquire enhanced migratory capacity might be the tumors microenvironment. As described above, GBMs frequently show necrotic areas surrounded by hypoxic regions. A study by Brat et al. (2004) indicates that hypoxia induces invasion and migration of glioblastoma cells. The study revealed, that this is, at least partially, caused by hypoxia induced mesenchymal transition of GBM cells (Brat et al. 2004).

1.1.3.2 Hypoxia in GBM

In several solid tumor entities, including high grade gliomas, tumor cells are exposed to hypoxic conditions which has an impact on the aggressiveness and therefore the prognosis of these tumors.

The development of hypoxic areas within tumors is a result of several mechanisms such as rapid cell proliferation, an increased O_2-dependend metabolism in cancer cells and the insufficient neovascularization for oxygen and nutrient supply for the tumor bulk.

Hypoxic conditions seem to affect the expression of several different genes. It was shown that hypoxia plays an important role for the maintenance of CSCs, the tumors therapy resistance and the development of migration and invasion capability (Karsy et al. 2016).

1.1.4 Tumorigenesis

Until now, tumorigenesis in human beings is not fully understood. The two main theories which are discussed to be responsible for gliomagenesis are the cancer stem cell theory, also called the hierarchical model and the stochastic model of tumorigenesis (s. Figure 1.2 and Figure 1.3).

Abundant evidence indicates that there is a minor subpopulation of cells in different cancer types, which exhibit stem cell properties like immortality, self-renewal capacity and the potential to differentiate into multiple cell lines by asymmetric division (Galli et al. 2004, Kreso and Dick 2014). In the cancer stem cell model, only the so-called cancer stem cells (CSCs) have the ability, to initiate tumor growth. CSCs are discussed to be responsible for tumor initiation, heterogeneity of cells within tumors, therapy resistance of tumors and tumor relapses after treatment (Galli et al. 2004, Bao et al. 2006, Sundar et al. 2014).

The existence of CSCs was first described in leukemia (Bonnet and Dick 1997) and in the following in several solid tumor entities, e.g. breast cancer (Al-Hajj et al. 2003), pancreatic cancer (Li et al. 2007) and different brain cancers (Galli et al. 2004).

Cells with stem cell properties in GBM were identified by using stem cell markers such as the cell surface antigens CD133 (Singh et al. 2004), SOX-2 (Berezovsky et al. 2014), CD44 (Anido et al. 2010), Nestin (Bexell et al. 2009) and more recently by the expression of ALDH1 (Rasper et al. 2010, Jin et al. 2013).

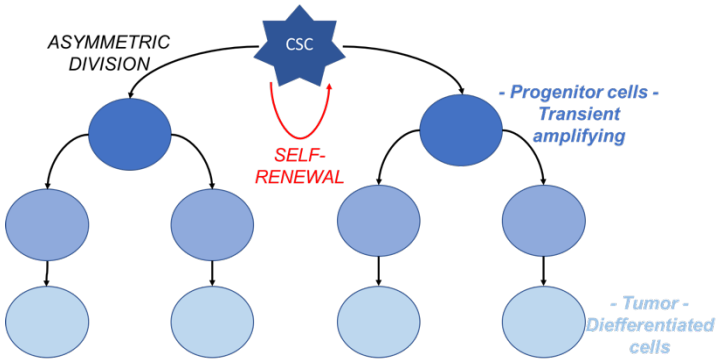

Figure 1.2 Cancer stem cell theory – Hierarchical model: Cells within tumors can be hierarchically organized, ranging from highly differentiated, less proliferative cells to almost undifferentiated, highly proliferative cells.

The stochastic model of tumorigenesis suggests, that tumors consist of biological homogenous cells. All cells have the potential to found new tumors. The functional heterogeneity of these cells is due to different intrinsic or random extrinsic influences. Due to the stochastic model, tumor growth follows the rules of Darwinian evolution. Cells with survival advantages maintain tumor growth and potentially resistance to therapies (Dick 2009, Sundar et al. 2014).

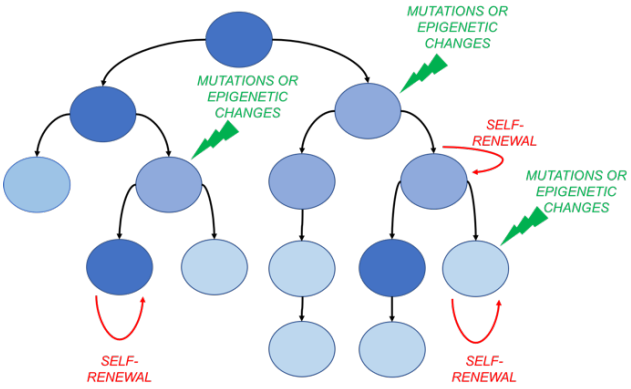

Figure 1.3 Stochastic model of tumorigenesis

Both theories, the hierarchical and the stochastic model, may play a role in development and maintenance of GBM. Targeting both kinds of GBM cells – the normal tumor cells as well as the GBM cancer stem cells (GCSCs) – might be the key to achieve sufficient treatment response in GBM patients.

1.1.5 Clinical presentation

The clinical presentation of GBM patients can differ depending on the tumors´ location. Due to the rapid growth, GBM can lead to elevated intracranial pressure. Increased intracranial pressure can cause headache, vomiting and impaired conciseness. Tumor related brain tissue necrosis can lead to focal neurological deficits. Other GBM patients show seizures, brainstem symptoms and cognitive and behavioural symptoms (Rees et al. 2016).

To diagnose GBM, MRI and CT imaging is used. GBM can appear as a ring-enhancing lesion which can show intratumoral necrosis or haemorrhage. These features lead to a heterogeneous appearance of the tumor in imaging. Figure 1.4 shows an example for a MRI image which is typical for GBM.

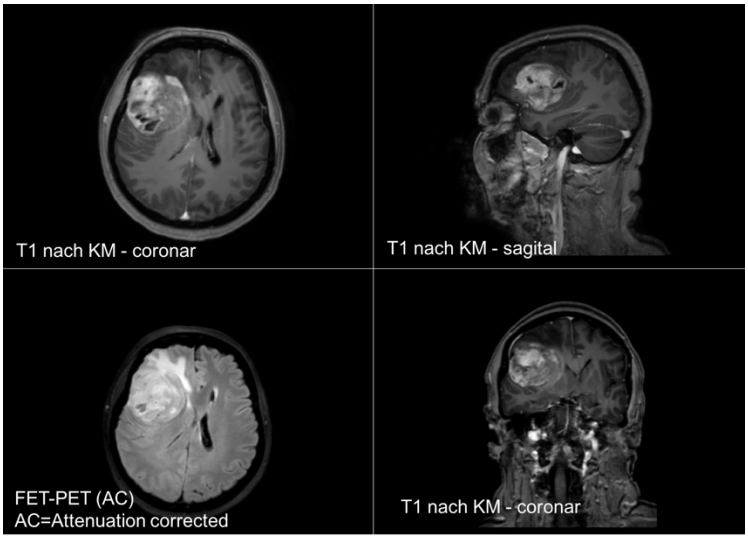

Figure 1.4 Glioblastoma multiforme in the right frontotemporal lobe. Thankfully obtained by Dr. med. Christoph Straube, Department of Radiation Oncology, Technical University of Munich (TUM), Germany.

1.1.6 Treatment and therapy resistance

The treatment-options for newly diagnosed glioblastoma include surgery, chemotherapy and radiotherapy. The decision which patient receives which kind of therapy depends on different factors like the patients´ age and clinical performance status, the tumor´s gene expression pattern and the tumor location (Komission Leitlinie der Deutschen Gesellschaft für Neurologie; S2k Leitlinie: für Diagnostik und Therapie in der Neurologie, Gliome; Aufl. 5, 2012, Addendum 01.03.2014).

Current standard of care in newly diagnosed GBM is based on a study published in 2005 by the European Organisation for Research and Treatment of Cancer (EORTC) and the National Cancer Institute of Canada Clinical Trials Group (NCIC) (Stupp et al. 2009). The so-called “Stupp regimen” includes surgery and radiotherapy of the resection cavity combined with a temozolomide (TMZ) chemotherapy followed by adjuvant TMZ alone.

For the treatment of recurrent tumors, there is no standardized therapy regimen. Currently, treatment strategies for recurrent GBM seem to vary widely in different therapy centers. Most agreed recommendation for therapy of relapsed tumors seems to be best supportive care (Hundsberger et al. 2016).

Despite these therapy options, GBM prognosis remains poor. One main problem in GBM treatment is therapy resistance which leads to GBMs´ poor prognosis. Especially relapsed tumors show increased therapy resistance. In the last decades, various causes for therapy resistance in GBMs were identified and intense research was done to understand the mechanisms behind therapy resistance in GBMs. Nevertheless, many questions in this field are not solved yet.

1.1.6.1 Surgery

The essential step in GBM treatment is surgery. On the one hand, it allows histological confirmation of the diagnosis and further histopathological investigations of the tumor tissue. On the other hand, it is important for cytoreduction and in some cases to reduce tumor associated symptoms such as elevated intracranial pressure or focal deficits.

Still, there are some limiting factors for surgical interventions in GBM patients, namely: poor performance status, advanced age or tumor infiltration of eloquent brain areas. Moreover, only a resection of about 80% of the tumor mass provides benefits for oncological treatment. (Wilson et al. 2014, Rees et al. 2016)

1.1.6.2 Radiotherapy and Radioresistance

After surgical tumor resection, external beam irradiation of the tumor cavity and 1-3 cm of the tumor margins is performed if possible. Radiotherapy usually is combined with TMZ chemotherapy. The standard dose for GBM patients is 60 Gy in total, delivered in 30 single doses of 2 Gy. If necessary, hypo fractioned regimens can be used for patients with low performance status (Bush et al. 2017).

Some studies could show, that x-ray irradiation improves overall survival (OS) and disease free survival (DFS) in elderly GBM patients (Scott et al. 2011) as well as OS and DFS of younger GBM patients. Although, other studies could only show slightly improvements of prognosis through radiotherapy (Keime-Guibert et al. 2007).

Unfortunately, the efficacy of radiation is limited by radioresistance of the tumor and radiation tolerance of the surrounding normal tissue.

Radioresistance is a main problem for GBM first-line therapy and even more for the therapy of relapsed tumors. Growing evidence leads to the assumption that radioresistance is mainly due to the existence of GBM cancer stem cells. GCSCs are less sensitive to radiotherapy than normal tumor cells. Several mechanisms which might be responsible for radioresistance in GBM stem cells are summarized in Figure 1.5.

GCSCs show the ability to reconstitute the tumor after treatment. Additionally, recurrent tumors show even increased radioresistance, which may be due to irradiation-induced CSC enrichment (Bao et al. 2006, Dahan et al. 2014).

Furthermore, research has shown, that especially hypoxia leads to enhanced radioresistance. Hypoxic areas within tumors are less sensitive to radiotherapy than normoxic regions, which is due to the fact, that a main effect of radiotherapy is the generation of reactive oxygen species (ROS) from intracellular water and molecular oxygen. ROS induce DNA damage and thus cell death. Hence, in the absence of O_2 radiotherapy is less effective. In addition, hypoxic conditions enhance the number of GCSCs within a tumor and GCSCs can be found more frequently in hypoxic areas (Heddleston et al. 2009, Soehngen

et al. 2014). In line with this, Soehngen et al. (2014) could prove upregulation of ALDH1 expression, which is a stem cell marker in GBM cells, after incubating GBM cells under hypoxic conditions.

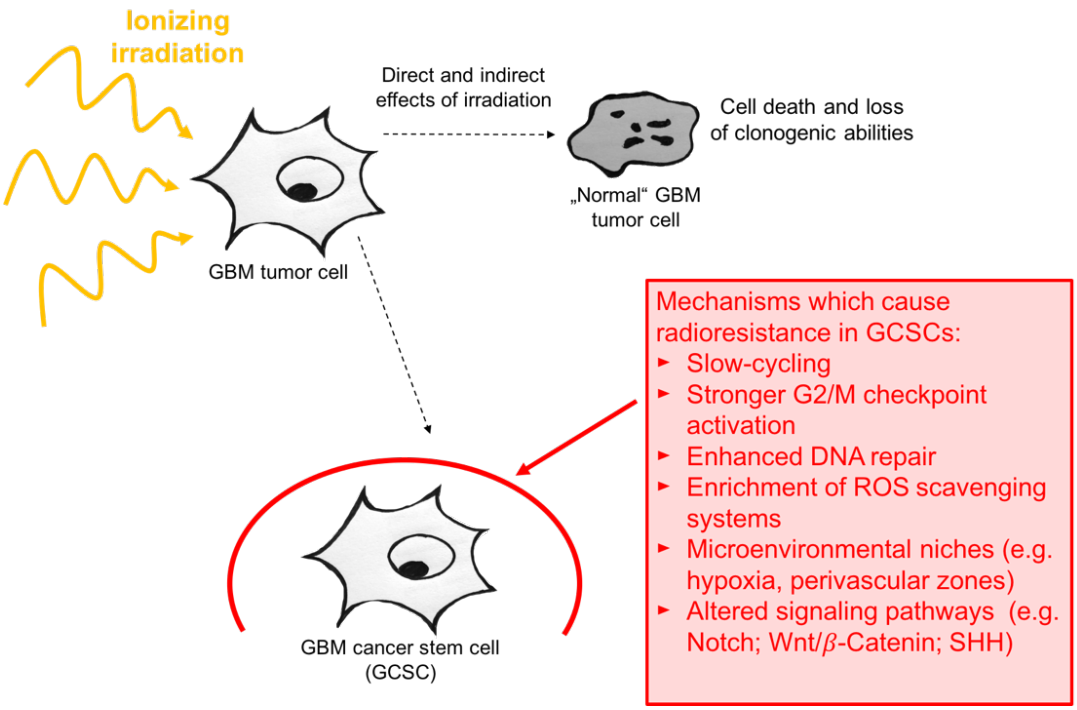

Figure 1.5 Mechanisms of radioresistance in GBM cancer stem cells (GCSCs) modified from (Kelley et al. 2016). (ROS, reactive oxygen species; Wnt, "Wingless/Integrated"; SHH, sonic hedgehog).

1.1.6.3 Chemotherapy and Chemoresistance

For a long time GBMs were considered being almost entirely resistant against chemotherapies. That is amongst others due to the blood-brain-barrier, which makes it difficult for chemotherapeutics to reach the tumor mass. Some tumor cells also have intrinsic mechanisms such as the expression of DNA damage repair proteins or dysregulation of apoptosis regulating genes (Sarkaria et al. 2008, Chacko et al. 2013).

Since a phase III trail from the European Organisation for Research and Treatment of Cancer (EORTC) and the National Cancer Institute of Canada Clinical Trials Group (NCIC) revealed in 2005, that GBM patients benefit from additional chemotherapy during radiotherapy with the alkylating agent temozolomide (TMZ), standard of care in GBM treatment includes chemotherapy with TMZ 6 weeks during and 6 weeks after radiotherapy (Stupp et al. 2005). An important prognostic factor for the success of chemotherapy with TMZ is the methylation status of the O^6-methylguanin-DNA-transferase (MGMT) gene promoter sequence. The MGMT gene encodes the DNA-damage repair protein MGMT which removes alkyl groups, amongst others, from O^6-guanin. Because alkylating O^6-guanin is one of the most important mechanisms for the effect of TMZ-treatment, methylation and therefore low expression and activity of MGMT makes TMZ treatment more effective (Hegi et al. 2005). Nevertheless, only

for GBM patients older than 60 years, studies could confirm a benefit through TMZ treatment for overall survival and progression free survival (Combs et al. 2011).

In the last years, several other chemotherapeutics have been tested in GBM patients, e.g. the implantation of dissolvable chemotherapy wafers (Gliadel®) in the tumor bed after surgery (Hart et al. 2011) or administration of the recombinant humanized VEGF (vascular endothelial growth factor) antibody bevacizumab (Avastin®) (Khasraw et al. 2014). Unfortunately, these approaches in GBM chemotherapy remained without huge improvements for OS of GBM patients (Ramirez et al. 2013).

1.2 ALDH1A1

1.2.1 ALDH superfamily

The ALDH (aldehyde dehydrogenase) superfamily consists of 19 yet known NAD(+) or NADP(+) dependent enzymes which are assigned to 11 families and 4 subfamilies. ALDHs are disseminated in several cellular compartments such as cytoplasm, nucleus, mitochondria and endoplasmatic reticulum (Sladek 2003, Xu et al. 2015).

ALDHs have several functions, which are important for cellular homeostasis. ALDHs play an important role in detoxification of endogenous and exogenous produced aldehydes. The enzymes of the ALDH superfamily oxidize aldehydes to their corresponding carboxylic acid. Thus, ALDHs are involved in alcohol metabolism by the oxidation of acetaldehyde.

Moreover, the ALDH enzymes play a role in the synthesis of retinoic acids (RA). Physiologically retinoic acids are important for embryogenesis and development. It was shown that RAs play an important role for the maintenance of CSCs and their properties (Niederreither et al. 2002, Moreb et al. 2017). Especially the subtypes ALDH1A1 and ALDH1A3 are regarded as consistent molecular markers for CSCs and as potential targets for cancer therapies.

Another important role of ALDHs is the clearing of toxic aldehydes derived from lipid peroxidation induced by reactive oxygen species (ROS) (Duester 2000, Vasiliou and Nebert 2005, Xu et al. 2015).

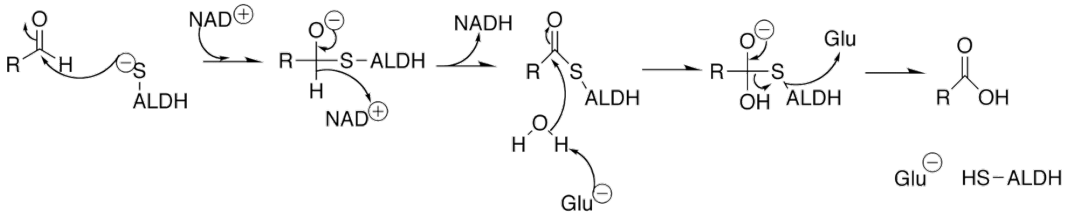

Figure 1.6 The reaction catalyzed by ALDH. Aldehydes get oxidized to their corresponding carboxylic acid.

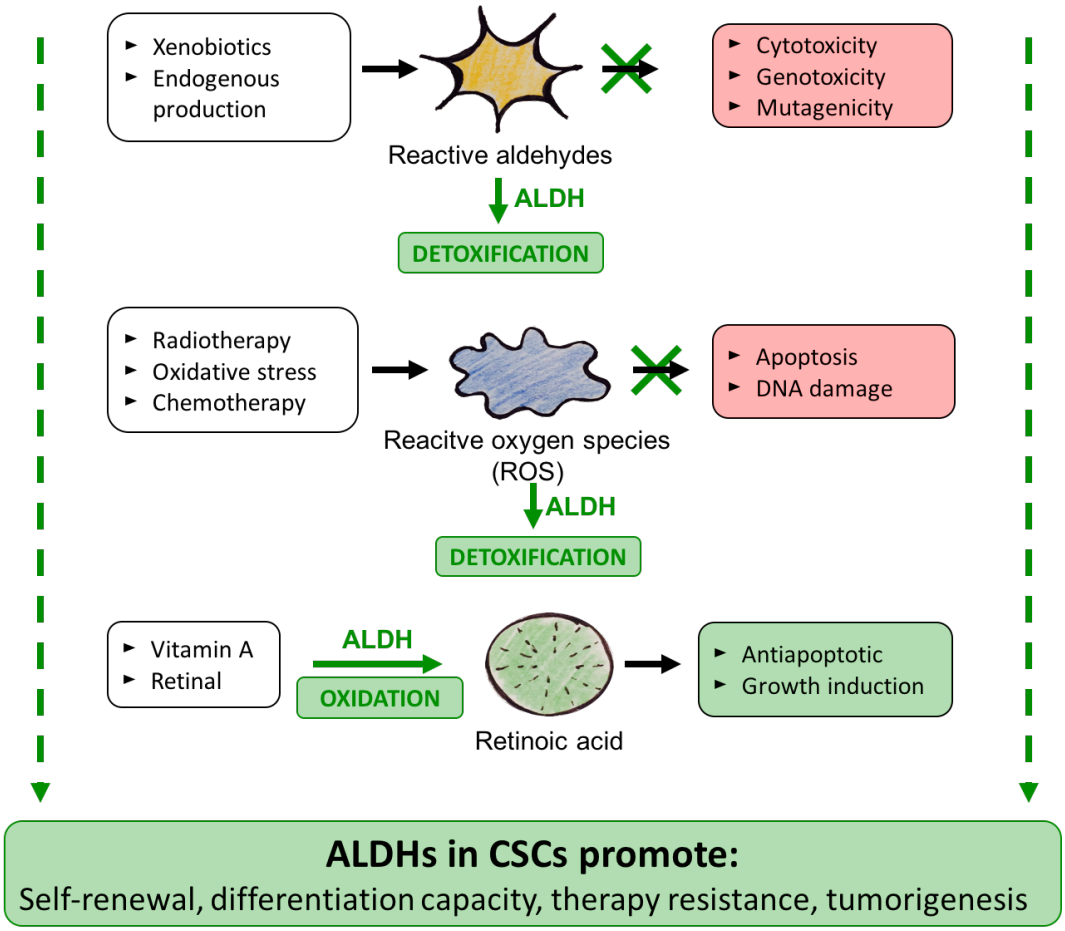

Figure 1.7 The function of ALDHs (aldehyde dehydrogenase) in CSCs (cancer stem cells) (Duester 2000, Vasiliou and Nebert 2005, Xu et al. 2015)

1.2.2 ALDH1A1

Aldehyde dehydrogenase 1 A 1 (ALDH1A1), also known as retinaldehyde dehydrogenase 1 (RADH1) is a cytosolic and mitochondrial NAD(+)-dependent enzyme. It is a homotetrameric protein with a molecular weight of 54kDa (Sladek 2003).

ALDH1A1 plays a pivotal role in alcohol metabolism, embryogenic development and differentiation as well as in detoxification of aldehydes, produced due to lipid peroxidation induced by ROS (reactive oxygen species) (Niederreither et al. 2002).

Recent research has shown, that high ALDH1A1 expression in gliomas is correlated with histological high-grade gliomas (III-IV) and therefore predicts poor prognosis. Xu et al. could show, that ALDH1A1 expression was elevated in invasive frontier areas of high grade gliomas and that high ALDH1A1 expression was correlated with strong invasiveness and high expression of matrix metalloproteinase 2, 7 and 9 (MMP2, MMP7, MMP9) which are important enzymes for cellular migration and tissue invasion.

Additionally, GBM patients who showed ALDH1A1 overexpression in normal brain tissue adjacent to the invasive frontiers had shorter disease free survival compared to patients without (Xu et al. 2015).

Furthermore, ALDH1A1 has been described as a marker for CSCs in leukemia (Hess et al. 2006) and several solid tumor entities such as breast cancer (Ginestier et al. 2007), lung cancer (Jiang et al. 2009), head and neck squamous cell carcinoma (Leinung et al. 2015), prostate cancer (Li et al. 2010), esophageal cancer (Yang et al. 2014) and GBM (Rasper et al. 2010). Most of the existing studies indicate, that ALDH1A1 expression is correlated with enhanced aggressiveness and poor prognosis of these tumors. Some studies could also show, that the expression of enzymes of the ALDH1-superfamily is correlated with radioresistance of tumor cells (Chen et al. 2009, Mihatsch et al. 2011). Furthermore, Schäfer et al. (2012) has shown, that ALDH1A1, plays a role in chemoresistance against TMZ, in GBM cells (Schäfer et al. 2012).

2 Objectives

Glioblastoma multiforme (GBM) is one of the most aggressive tumors in humans with a very poor prognosis. Even with the best up to date multimodal therapy, median survival is still very short with 15 months. Despite extensive research, only small advances have been made to improve overall survival and prognosis in GBM patients in recent decades.

One cornerstone of GBM treatment is radiotherapy. Though, most GBMs become resistant towards irradiation during therapy. The mechanisms, which lead to radioresistance in GBM cells are not fully understood yet.

Recent research point out, that the expression of enzymes of the ALDH1-superfamily is correlated with radioresistance and chemoresistance in GBM cells.

For these reasons, the main question of this study was: Does the expression of ALDH1A1, a member of the ALDH1 superfamily, affects radiosensitivity of GBM cells?

Another property that seems to be crucial for the tumors aggressiveness is cell-mobility. Migrating cells might be able to escape therapies and therefore lead to recurrence. Furthermore, the ability of cells to move leads to invasiveness, which is another important part that leads to tumors´ high malignancy.

Therefore, the second research question was: Does ALDH1A1 expression has an influence on the migratory capacity of GBM cells?

Up to date it is not known if there is any trigger for enhanced ALDH1A1 expression. GBM and several other high malignant tumor entities show hypoxic areas within the tumors. In these areas tumor cells seem to be more resistant towards therapies and show increased migratory capacity.

Soehngen et al. could show, that in hypoxic areas within the GBM tumor bulk, ALDH1A1 is overexpressed (Soehngen et al. 2014). Therefore, we explored**,** if hypoxia leads to enhanced ALDH1A1 expression?

All in all, the study´s final objective was to investigate the question: Could ALDH1A1 expression serve as a new prognostic marker in GBM patients and to go even further, could ALDH1A1 be a new target for GBM treatment?

3 Methods and Materials

3.1 Materials

3.1.1 Cell line

LN18 is a GBM cell line established 1976 in France. Cells were taken from a 61 years old white male patient out of a tumor, located at the right temporal lobe. The cell line was described and characterized in detail by Diserens et al. in 1981 (Diserens et al. 1981). Cells were thankfully obtained from the Neuro-Radiation Oncology Research Group, Department of Radiation Oncology, University Hospital of Heidelberg, Germany. LN18 was ID-typified by GATC Biotech AG.

3.1.2 Technical devices

Table 3.1 Technical devices

Device	***Model***	***Producer***
Centrifuges	Mega Star 3.0 R	VWR, Lutterworth, UK
	Heraeus™ Fresco™ 21 Micro-centrifuge	Thermo Fisher scientific, Waltham, USA
Colony counter	GelCount™	Oxford Optronix, Abingdon, UK
Flow cytometer	FACSCalibur™ flow cytometer	BD Biosciences, San Jose, USA
Gel Imaging System	ChemiDoc™ Touch Imaging System	Bio-Rad Laboratories Inc., Hercules, USA
Heat block	TB1 Thermoblock	Biometra GmbH, Göttingen, Germany
Hypoxia incubator	HypoxyLab™	Oxford Optronix, Abingdon, UK
Incubator	BBD 6220 CO2 Incubator	Thermo Fisher scientific, Waltham, USA
Laminar flow cabinet	Herasafe™ KS	Thermo Fisher scientific, Waltham, USA
Microplate reader	BioTek™ EL808™ Absorbance Microplate Reader	BIO-TEK Instruments, Inc., Winooski, USA
Microscope	ZEISS Primovert	Carl Zeiss Microscopy GmbH, Jena, Germany

Speed rotator	Intelli-Mixer RM-2L	ELMI, Calabasas, USA
Blotting chamber	Mini-PROTEAN® Tetra Cell 4-Gel System and Mini Trans Blot® Cell	Bio-Rad Laboratories, Munich, Germany
X-ray irradiation device	RS225A	Gulmay Medical Ltd., Surrey, UK

3.1.3 Software

Table 3.2 Software

Software	***Producer***
Axio Vision	Carl Zeiss Microscopy GmbH, Jena, Germany
BD CellQuest™	BD Biosciences, San Jose, USA
GelCount™	Oxford Optronix, Abingdon, UK
Gene 5™	BIO-TEK Instruments, Inc., Winooski, USA
Image Lab™	Bio-Rad Laboratories, Inc., Hercules, USA
ImageJ	Public domain
Microsoft Excel®	Microsoft Corporation, Redmond, USA
ModFit™ LT	Verity Software House, Topsham, USA
SigmaPlot	Systa Software, Inc., San Jose, USA

3.1.4 Chemicals and reagents

Table 3.3 Chemicals and reagents

Substance	***Abbreviation***	***Producer***
2-mercaptoethanol		Carl-Roth GmbH & Co. KG, Karlsruhe, Germany
AlamarBlue® reagent		Thermo Fisher Scientific, Inc., Rockford, USA
Amersham™ Full-Range Rainbow™ Molecular Weight Marker		(GE Healthcare Europe GmbH, Freiburg, Germany)

Bromphenol blue		Carl-Roth GmbH & Co. KG, Karlsruhe, Germany
Crystal violet 0.25%		Krankenhausapotheke Klinikum rechts der Isar, Munich, Germany
Dimethylsulfoxide	DMSO	Sigma-Aldrich Chemie GmbH, Steinheim, Germany
Dulbecco´s phosphate buffered saline	PBS	Sigma-Aldrich Chemie GmbH, Steinheim, Germany
Fetal bovine serum	FBS	Sigma-Aldrich Chemie GmbH, Steinheim, Germany
Glycerol		Sigma-Aldrich Chemie GmbH, Steinheim, Germany
Glycine		Carl-Roth GmbH & Co. KG, Karlsruhe, Germany
Hexadimethrine bromide, ≥94% (titration)		Sigma-Aldrich Chemie GmbH, Steinheim, Germany
Immobilon®-P Transfer Membrane pore size 0.45 µm		Millipore Corporation, Billerica, USA
Methanol	MeOH	Carl-Roth GmbH & Co. KG, Karlsruhe, Germany
Penicillin-Streptomycin	Pen/Strep	Sigma-Aldrich Chemie GmbH, Steinheim, Germany
phosSTOP™, Phosphatase inhibitor cocktail tablets provided in EASYpacks		Roche Diagnostics GmbH, Mannheim, Germany
cOmplete™ ULTRA Teblets, Mini, EDTA-free EASYpack, Protease Inhibito Cocktail Tablets		Roche Diagnostics GmbH, Mannheim, Germany
Pierce™ BCA Protein Assay Kit		Thermo Fisher Scientific, Inc., Rockford, USA

Phenylmethylsulfonylfluorid PMSF	PMSF	Sigma-Aldrich Chemie GmbH, Steinheim, Germany
Powdered milk, blotting grade		Carl-Roth GmbH & Co. KG, Karlsruhe, Germany
Puromycin dihydrochloride		Sigma-Aldrich Chemie GmbH, Steinheim, Germany
Propidium iodid	PI	Sigma-Aldrich Chemie GmbH, Steinheim, Germany
RNAse A		Sigma-Aldrich Chemie GmbH, Steinheim, Germany
Roswell Park Memorial Institute 1640 medium with L-glutamine and sodium bicarbonate	RPMI-1640	Sigma-Aldrich Chemie GmbH, Steinheim, Germany
Sodium dodecyl sulfate Pellets	SDS	Carl-Roth GmbH & Co. KG, Karlsruhe, Germany
Tetramethylethylendiamin	TEMED	Carl-Roth GmbH & Co. KG, Karlsruhe, Germany
Trishydroxymethylaminomethan	TRIS	Carl-Roth GmbH & Co. KG, Karlsruhe, Germany
Triton X-100		Sigma-Aldrich Chemie GmbH, Steinheim, Germany
Trypan blue		Sigma-Aldrich Chemie GmbH, Steinheim, Germany
Trypsin – EDTA Solution		Sigma-Aldrich Chemie GmbH, Steinheim, Germany
Tween® 20 detergent		Merck, Darmstadt, Germany

3.1.5 Consumables

Table 3.4 Consumables

Consumable	***Producer***
12 well plates	Sigma-Aldrich Chemie GmbH, Schnelldorf, Germany
96 well plates	TPP® Techno Plastic Products AG, Trasadingen, Switzerland
Cell scraper	TPP® Techno Plastic Products AG, Trasadingen, Switzerland
Cellstar® cell culture dishes 100/20 mm	Greiner Bio-One International GmbH, Frickenhausen, Germany
Cellstar® filter screw cap cell culture flasks, growth area 25, 75 and 165cm^2	Greiner Bio-One International GmbH, Frickenhausen, Germany
Cellstar® Serological pipettes 2, 5, 10, 25 and 50 ml	Greiner Bio-One International GmbH, Frickenhausen, Germany
Combitips advanced®, 0.1 and 0.5 ml	Eppendorf AG, Hamburg, Germany
Corning^{TM} Falcon^{TM} 15 and 50ml conical centrifuge tubes	Greiner Bio-One International GmbH, Frickenhausen, Germany
Culture-Insert 2 Well in µ-Dish 35mm, low ibiTreat	Ibidi GmbH, Munich, Germany
Eppendorf Safe-Lock Tubes, 0.5, 1.5 and 2 ml	Eppendorf AG, Hamburg, Germany
FACS Tubes 5ml	Sarstedt AG & Co, Nümbrecht , Germany
T311 – Cryovial®, 1.2 ml	Simport®, Beloeil, Canada

3.2 Methods

3.2.1 Cell culture

3.2.1.1 Cultivation

LN18 wildtype cells were cultured in RPMI 1640 medium supplemented with 10% heat-inactivated fetal bovine serum (FBS) and 1% penicillin-streptomycin (pen/strep). The medium for the transfected LN18 cell lines ALDH1A1- (LN 18 knockdown cells) and ALDH1A1+ (LN 18 control cells) also contained 4 µg/ml puromycin to maintain the ALDH1A1 knockdown. Cells were cultured under standard cell culture conditions at 37° C and 5% CO_2.

Cells were passaged usually twice a week when 70-80% confluent. Therefore, medium was removed from T75 cell culture flask. Cells were rinsed once with 10 ml PBS. 2 ml 0.05% trypsin-EDTA was added and cell culture flask placed in a 37° C incubator for approximately 4 min until cells were detached from the surface. After that, 6 ml medium was added (proportion medium to trypsin 3:1) to stop trypsin-activation.

Cells were counted using a Neubauer counting chamber. Usually $5x10^5$ cells were transferred to a new T75 cell culture flask and filled up to 15 ml with medium.

3.2.1.2 Freezing and thawing frozen cells

For cryopreservation, cells were stored in liquid nitrogen using a freezing medium consisting of 65% RPMI 1640, 25% FBS and 10% dimethylsulfoxide (DMSO). Cells were stored in 2 ml cryo vials in a concentration of 1 x 10^6 cells/ml.

To thaw frozen cells, cryo vials were removed from liquid nitrogen and immediately placed into a 37° C water bath. Cells were quickly (< 1 min) thawed under gently swirling of the vial in the water bath. 1 ml of complete growth medium was added to the cell solution under sterile conditions. Vial content was transferred into a 15 ml Falcon™ tube containing 9 ml pre-warmed complete growth medium. Tube was centrifuged for 5 min and 1000 rpm. After centrifugation supernatant was discarded and the pellet resuspended in 15 ml complete growth medium. Cell suspension was transferred into a T75 cell culture flask and kept in culture.

3.2.2 ALDH1A1 knockdown with shRNA

ALDH1A1 knockdown in GBM cell line LN18 was done using lentiviral transduction with shRNA (short hairpin RNA) (s. Figure 3.1).

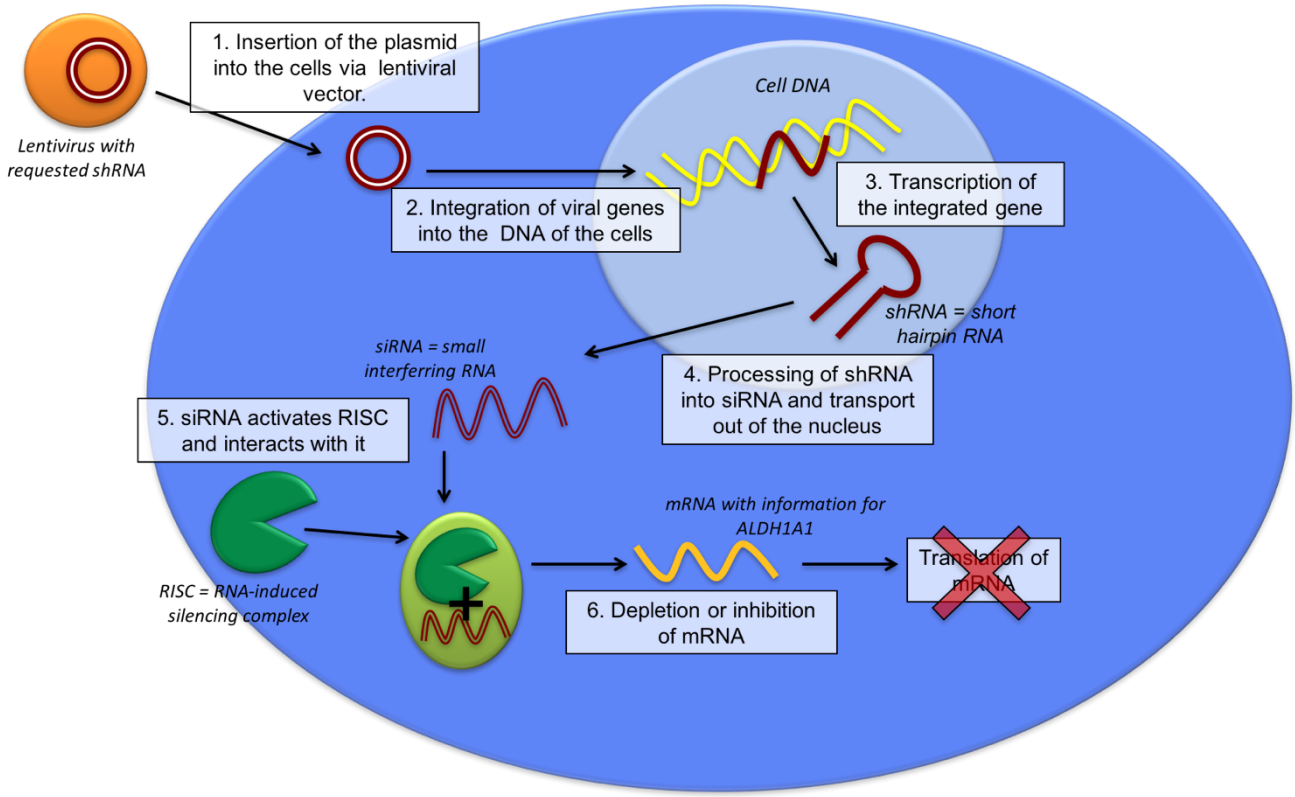

Figure 3.1 Schematic overview of the intracellular processes due to lentiviral transduction.

3.2.2.1 Puromycin titration (kill curve)

To select LN18 cells with stable knockdown after transduction the antibiotic puromycin was used as selective agent. To find the appropriate concentration of puromycin for selection of stable cell lines, a puromycin titration was performed with non-transduced LN18 cells.

Therefore, LN18 cells were plated into a 96 well plate (4000 cells per well). After incubation for 24 h at 37° C and 5% CO_2 medium was removed and 200 µl of fresh medium, containing 0.5-10 µg/ml puromycin was added. Cells were treated in triplicates with different puromycin concentrations. Cell viability was examined microscopically every day. Medium containing puromycin was replaced every 3 days for 2 weeks.

3.2.2.2 Lentiviral transduction

For ALDH1A1 knockdown, MISSION® Lentiviral Transduction Particles, clone TRCN0000026415 (NM ID NM_000689), was obtained from Sigma-Aldrich, Inc., St. Louis, USA. For mock control MISSION® Non-Mammalian shRNA Control Transduction Particles, also received from Sigma-Aldrich, Inc., St.

Louis, USA, were used. Lentivirus Transduction Particles were stored at -70°C as recommended by the product information.

Name	Description
U6	U6 Promoter
cppt	Central polypurine tract
hPGK	Human phosphoglycerate kinase eukaryotic promoter
puroR	Puromycin resistance gene for mammalian selection
SIN/3´LTR	3´self inactivating long terminal repeat
f1 ori	f1 origin of replication
ampR	Ampicillin resistance gene for bacterial selection
pUC ori	pUC origin of replication
5´LTR	5´long terminal repeat
Psi	RNA packaging signal
RRE	Rev response element

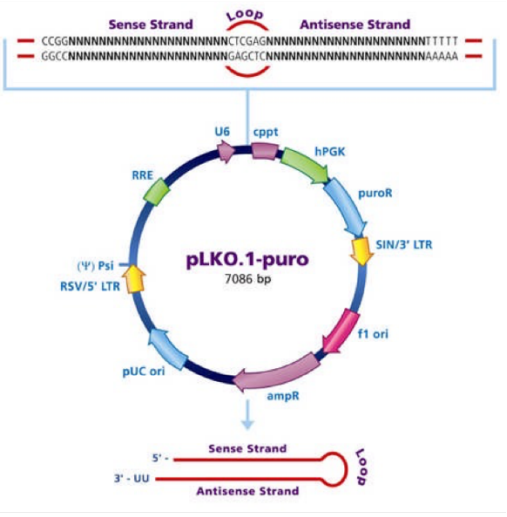

Figure 3.2 TRC1 and TRC1.5 Lentiviral Plasmid Vector pLKO.1-puro Features. Source: Sigma-Aldrich, Inc., St. Louis, USA.

For transduction, $1.2x10^4$ cells per well were plated into a 96 well plate and incubated overnight. Medium was removed and 110 µl RPMI 1640 medium containing 8 µg/ml hexadimethrine bromide to enhance transduction, was added to each well. Slowly thawed MISSION® Lentiviral Transduction Particles and MISSION® Non-Mammalian shRNA Control Transduction Particles were added drop-wise in triplicates at different MOIs (Multiplicity of Infection = number of transducing lentiviral particles per cell). MOI of 1, 2, 5 and 10 were used. Cells were incubated overnight. After 24 h medium was removed and 110 µl fresh RPMI 1640 medium without puromycin added and cells were again incubated overnight. After 24h medium was removed and 110 µl fresh medium, containing 4 µg/ml puromycin was added. Medium was changed every 2 days. 8 days after transduction, cells were transferred into 24 well plates and finally, after 16 days and some intermediate steps (12 well plate, 6 well plate, T25 cell culture flask) passaged into T75 cell culture flasks.

Cells were then analyzed for ALDH1A1 knockdown on protein level, performing Western blot analysis as described below. Successful knockdown clones were maintained in RPMI 1640 medium containing 4µg/ml puromycin to sustain stable knockdown.

3.2.3 Western blot analysis

Western blot analysis was performed to detect ALDH1A1 expression in GBM cell lines on the protein level.

3.2.3.1 Buffers and solutions

Table 3.5 Buffers and solutions

Lysis buffer; Radioimmunoprecipitation assay (RIPA) buffer	150 mM NaCl, 1% Triton X-100, 50 mM Tris pH 8, 0.5% Sodium deoxycholate, 0.1% SDS
Lämmli sample buffer	4% SDS, 10% 2-mercaptoethanol; 20% glycerol; 0,004% bromphenol blue; 0.125 M Tris-HCl pH 6.8;
Running buffer	250 mM Tris, 1.9 M Glycine, 10% SDS
Transfer buffer	250 mM Tris, 1.9 M Glycine, 20% MeOH
Blocking buffer	5% dried milk in PBS-T
Washing buffer (PBS-T)	1x PBS, 0.1% Tween-20

3.2.3.2 Protein isolation and determination

Cells were cultured for 48 h in cell culture dishes (10 cm diameter) until the monolayer was approximately 70% confluent. For cell lysis culture dishes were placed on ice and medium was removed. Cells were rinsed with 5 ml PBS. 150 µl RIPA buffer supplemented with 1 mM PMSF, phosphatase and protease inhibitors, was added. Adherent cells were scraped off the dish using a plastic cell scraper. Cell suspension was transferred into a precooled 500 µl Eppendorf-tube. Tubes were put on ice for 30 min and then spun at 14000 rpm for 10 min in a 4° C precooled centrifuge. Supernatant was transferred into 150 µl Eppendorf-tubes and stored at -20° C.

The protein amount was determined by using the Pierce™ BCA Protein Assay Kit (Thermo Fisher Scientific, Rockford, USA). Colorimetric detection and quantitation of the total protein was performed using a microplate reader and the software Gene5™ (BioTek, Winooski, USA).

3.2.3.3 SDS-Page (Sodium dodecyl sulfate polyacrylamide gel electrophoresis)

Table 3.6 Gel preparation for SDS-Page

	5% stacking gel (2.5175 ml ≙ 1 gel)	***10% separating gel (5.002 ml ≙ 1 gel)***
H_2O	1.4 ml	2.0 ml
30% Acrylamide	415 µl	1.65 ml
0.5 M Tris pH6,8	650 µl	
1.5 M Tris pH8		1.25 ml
10% SDS	25 µl	50 µl
10% APS	25 µl	50 µl
TEMED	2.5 µl	2 µl

Following the results of the protein determination, equal amounts of protein (25 µg per sample) were separated by SDS-PAGE.

Therefore, protein samples were diluted with lysis buffer (RIPA buffer). Lämmli sample buffer in a proportion of 1:3.3 was added. The samples were heated for 10 min to a temperature of 95° C to promote protein denaturation and SDS binding.

Protein separation was done at 120 V and 10mA for 1.5 – 2 h using a Mini-PROTEAN® Tetra cell 4-gel system (Bio-Rad Laboratories, Munich, Germany). Gels for protein separation were prepared as described in Table 3.6. An Amersham™ full-range Rainbow™ molecular weight marker (GE Healthcare Europe GmbH, Freiburg, Germany) was used for protein size determination on the SDS polyacrylamide gels.

3.2.3.4 Western blotting

After SDS-PAGE proteins were transferred to a polyvinylidene difluoride (PVDF) membrane through tank blotting using the Mini-PROTEAN® Tetra Cell combined with the Mini Trans Blot® Cell (Bio-Rad Laboratories, Munich, Germany). For transfer, a fitting piece of PVDF membrane was cut out and incubated in MeOH for a few seconds. The transfer sandwich was assembled as shown in Figure 3.3.

The cassette, together with an ice block, were placed in the transfer tank. The tank was filled with transfer buffer up to the given marking. The transfer was done for 1 h at 90 V.

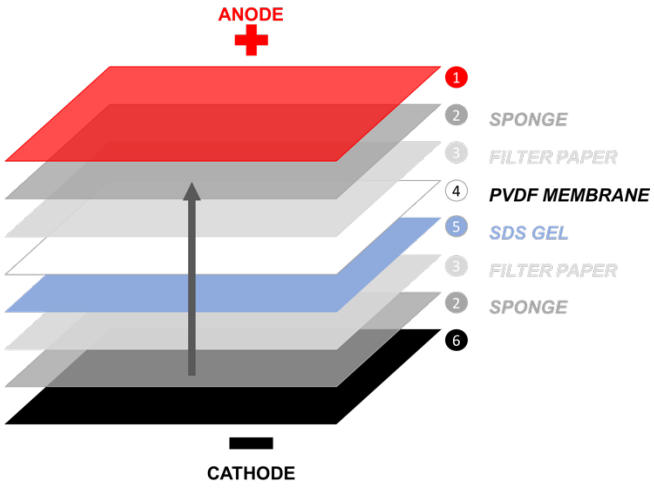

Figure 3.3 Schematic structure of tank blot system for protein transfer from gel to PVDF membrane

To prevent nonspecific binding of antibodies, the membrane was blocked in 5% dry-milk in PBS-T for 1 h at room temperature. Afterwards, the membrane was incubated overnight at 4° C with primary antibody, diluted in 5% dry-milk (dilution see Table 3.7).

After overnight incubation, the blot was rinsed 3 times for 10 min with PBS-T and then incubated for 1h at room temperature with the secondary antibody. The secondary antibody was diluted in 5% dry-milk (dilution see Table 3.7). The blot was again rinsed 3 times for 10 min with PBS-T.

To develop the blot, SuperSignal™ West Femto Maximum Sensitivity Substrate (Thermo Fisher Scientific, Rockford, USA), an enhanced chemiluminescent (ECL) substrate was used and the chemiluminescent signals detected via ChemiDoc™ Touch Imaging System (Bio-Rad Laboratories, Munich, Germany).

To show if samples have been loaded equally and if proteins from the samples were transferred to the membrane, β-Actin, an ubiquitous expressed protein in human cells, was used as loading control. Hence, the membrane was rinsed 3 times for 10 min with PBS-T after detection of ALDH1A1. The membrane was incubated overnight at 4° C with β-Actin primary antibody diluted in 5% dry-milk (dilution s. Table 3.7). After overnight incubation the blot was rinsed 3 times for 10 min with PBS-T and then incubated for 1 h at room temperature with the secondary antibody.

Detection of β-Actin was performed as described above.

Table 3.7 Antibodies

Primary antibodies

Antibody	***Clone***	***Dilution***	***Producer***	***Catalog number***
Aldehyde Dehydrogenase 1-A1/ALDH1A1-antibody (Mouse)	# 703410	1:500	R&D Systems Inc., Minneapolis, USA	MAB5969
Monoclonal Anti-β-Actin antibody (Mouse)	AC-74	1:2500	Sigma-Aldrich, St.Louis, USA	A5316
Carbonic Anhydrase IX/CA9-antibody (Mouse)	LS-B273	1:1000	LifeSpan BioScience, Inc., Seattle, USA	LS-C35269-100
HIF1α-Antibody (Mouse)	MAB1536	1:500	R&D Systems Inc., Minneapolis, USA	MAB 1536

Secondary antibodies

Antibody	***Clone***	***Dilution***	***Producer***	***Catalog number***
Anti-Mouse IgG (H+L), HRP conjugate		1:2500	Promega Corporation, Madison, USA	W4028

3.2.4 Clonogenic assay

Clonogenic assay also called colony formation assay, is a common method to investigate radiosensitivity of cells and cell survival after irradiation or treatment with other potentially cytotoxic agents. The assay is based on the capacity of a single, the treatment surviving cell to divide and to grow into a colony.

Therefore, cells were seeded into 12 well plates after precise counting in a concentration as described in Table 3.8 in 2 ml medium per well. Cells were incubated overnight. Cells were irradiated with 0, 2, 4, 6 or 8 Gy (for details s. 3.2.7). Following 12 days, when cells had formed colonies, consisting of at least 50 cells, medium was removed. Colonies were washed 1 time with PBS and fixed with 1 ml cold MeOH

per well for 5 min. MeOH was removed and colonies were stained with 1 ml crystal violet (0.25%) per well for 2 min. After staining, plates were rinsed with water.

Pictures of the plates were taken with the colony counter GelCount™ (Oxford Optronix Ltd., Abingdon, UK). Colonies were counted manually based on the pictures using the GelCount™ software (Oxford Optronix Ltd., Abingdon, UK).

Cell survival curves were fitted to the linear quadratic model (formula: $S = e^{-(\propto D + \beta D^2)}$), using the software Sigmaplot (Systa Software, Inc., San Jose, USA)

Table 3.8 Seeded cell numbers for CFA

Irradiation (Gy)	***Seeded cells per well***
0	200
2	600
4	600
6	1000
8	2000

3.2.5 Migration assay / Wound healing assay

Migration capacity of ALDH1A1- cells and ALDH1A1+ cells and migration of these cells after irradiation was investigated by wound healing assays. Wound healing assays were done using Ibidi® culture inserts 2 well.

$6x10^5$ cells per well were seeded in 70 µl RPMI 1640 medium supplemented with 10% FCS, 1% Pen/Strep and 4 µg/ml puromycin into culture inserts 2 well µ-dishes (35 mm; Ibidi®). Cells were incubated under usual conditions (5% CO_2, 37° C) for 24h so that cells reach almost 100% confluence as a monolayer. Cells were irradiated with 0, 2 or 8 Gy (for details see Table 3.8). After irradiation, medium was removed and cells were rinsed with PBS. Silicon culture insert was removed, leaving a 500 µm cell free gap. 2 ml fresh medium per culture dish was added. Medium was this time supplemented with only 0.1% FCS to prevent cell proliferation. Pictures of the cell free gaps were acquired under bright-field microscope (10x magnification) immediately and 6, 24, 30 and 48 h after irradiation.

Pictures were analyzed by measuring the cell free area within the initially 500 µm cell free gap using the ImageJ wound healing tool.

3.2.6 Proliferation assay

The alamarBlue® proliferation assay was performed to explore proliferation of ALDH1A1+ and ALDH1A1- cells. The alamarBlue® reagent (Thermo Fisher Scientific, Rockford, USA) contains resazurin, a nontoxic, cell permeable blue substance. After entering the cell, resazurin is reduced by the cells metabolic activity to resorufin, which changes the color of alamarBlue® into red. For this reason, alamarBlue® reduction in cells is an indicator for cell proliferation. The color change was measured using spectrophotometry.

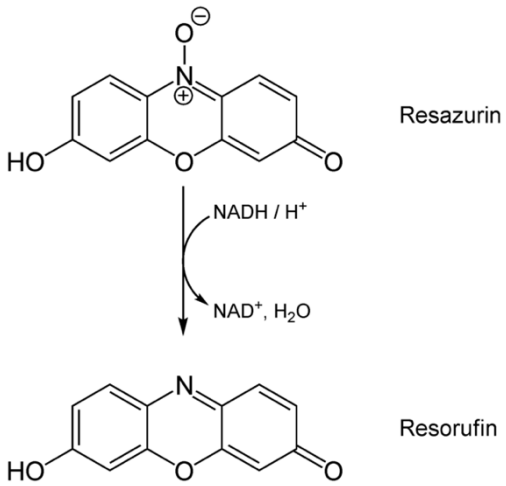

Figure 3.4 Chemical reaction of alamarBlue®. Resazurin, which is non-fluorescent, is converted to redfluorescent Resafurin due to cells´metabolism.

In detail, ALDH1A1+ and ALDH1A1- cells were seeded into 4 96 well plates (one plate for one measurement time-point as described below). Different numbers of cells per well were seeded (125, 250, 500, 1000, 2000, 4000 cells per well) in100 µl RPMI 1640 medium per well. Of every cell number, triplicates were seeded. Medium without cells was used as blank.

After seeding, cells were incubated under usual conditions.

Proliferation was determined at the time points 24, 48, 72 and 96h after seeding. Therefore, at every time point 10 µl alamarBlue® was added to seeded cells and incubated for 4 h at 37° C. After 4 h absorbance was measured at two different wavelengths (570 nm and 630 nm), using the microplate reader BioTek™ EL808™ (BIO-TEK Instruments, Inc., Winooski, USA) and the software Gene5. Absorbance at 630 nm was taken as reference value and subtracted from absorbance values at 570nm. The measured blank value was also subtracted.

Doubling time (t_d) was calculated mathematically, using the formula $t_d = \frac{\ln(2)}{k}$, with growth constant k, which was determined by graphical analysis of the growth curve.

3.2.7 Analysis of cell cycle distribution

Cell cycle analysis of ALDH1A1+ and ALDH1A1- cells 24h after X-ray irradiation was done by flow cytometry. Degradation of RNA by RNase and staining of DNA with PI allows to quantify the DNA amount within cells during different phases of cell cycle (cell cycle phases: G0, G1, S, G2 and M).

For cell cycle analysis $6x10^5$ ALDH1A1+ and ALDH1A1- cells were seeded in 10 cm cell culture dishes and incubated under usual conditions (5% CO_2, 37°C) for 24 h. After 24 h, when cells showed 50% confluence in the monolayer, cells were irradiated with 0, 4 and 8 Gy, using the X-ray device RS225 (Gulmay Medical, Surrey, UK). Afterwards cells were again incubated for 24 h.

24h following irradiation, cells were collected by trypsinization. Cell suspension was spun at 500 g for 5 min in a 4° C precooled centrifuge. Supernatant was discarded and cell pellet resuspended in 250 µl precooled PBS. Suspension was transferred dropwise into 2,25 µl -20°C precooled 70% ethanol while vortexed. Cells were stored at least for 2 h at -20°C.

Table 3.9 Propidium iodide staining solution

Reagent	***Concentration***
0,1% Triton X-100 in PBS	0,1%
DNAse-free RNAse A (Thermo Fisher Scientific, Inc., Rockford, USA)	0,2 mg/ml
Propidium iodide (PI) (Thermo Fisher Scientific, Inc., Rockford, USA)	0,02 mg/ml

For DNA staining, PI staining solution was prepared as described in Table 3.9 and kept at 4°C in the dark. Cells in ethanol were centrifuged for 5 min at 500 g in a 4°C precooled centrifuge. Ethanol was discarded and cell pellet resuspended in 500 µl PI staining solution and incubated for 1 h under room temperature in the dark.

Cell cycle was analyzed with FACSCalibur™ flow cytometer (BD Biosciences, San Jose, USA) with 10000 events per determination. Fluorescent signals were detected with FL2 laser. ModFit® software (Verity Software House, Topsham, USA) was applied for detailed analysis.

3.2.8 Irradiation

X-ray irradiation of cells was delivered by the X-ray device RS225 (Gulmay Medical, Surrey, UK). The dose rate was 1 Gy per 1.07 minutes, voltage was set at 200 kV and 15 mA. For irradiation, all cells which were investigated in an experiment, were taken out of the incubator for the same time span.

3.2.9 Hypoxia

Cells were cultivated under hypoxic conditions using the bench top hypoxia workstation (HypoxyLab™, Oxford Optronix, UK). An atmosphere containing a mixture of 95% nitrogen, 5% CO_2 and an oxygen concentration of 1% O_2, was generated. The temperature was held at a usual level of 37° C.

To investigate the effect of hypoxia on the ALDH1A1 expression in ALDH1A1+ and ALDH1A1- cells, 35 x 10^4 cells were seeded per 100/20 mm cell culture dish and cultured under usual conditions. After 24 h medium was removed and fresh medium was added. Afterwards cells were incubated under hypoxic conditions for 24 h and lysed with RIPA buffer (s. Table 3.5) within hypoxic conditions.

3.2.10 Statistics

Except Western Blot analysis, all assays were performed at least 3 times. Data were analyzed using the software Sigmaplot and Microsoft Excel® and data point stated as mean ± SEM (Standard error of the mean). Unpaired t-test was used to generate p-values. $P<0.05$ was considered statistically significant and marked with *, $p<0.01$ with ** and $p<0.001$ with ***, in diagrams.

4 Results

4.1 Generation of stable ALDH1A1 knockdown in GBM cell line LN18

To investigate the impact of ALDH1A1 expression in GBM cells on its radiosensitivity and migratory capacity, GBM cell lines with different ALDH1A1 expression were needed. To obtain these cell lines, an ALDH1A1 knockdown in the ALDH1A1 expressing GBM cell line LN18 was performed by a lentiviral transduction using shRNA (short hairpin RNA) (see 3.2.2.2).

The cell line LN18 was chosen for transduction because ALDH1A1 expression could be detected in this cell line by Western Blot analysis in contrast to other tested GBM cell lines.

To select transducted cells from non-transducted ones, the antibiotic puromycin was used. To find the right concentration of puromycin for selection, killing of parental LN18 cells by different puromycin concentrations was investigated. The result was that the minimum concentration of puromycin that caused complete cell death in LN18 cells after 3-5 days was 4 µg/ml. Therefore, selection of transducted cells was performed with medium supplemented with puromycin in a concentration of 4µg/ml.

LN18 cells were transfected with two different lentiviral transduction particles, a lentiviral ALDH1A1 knockdown transduction particle and a lentiviral transduction particle only with a puromycin resistance gene and without ALDH1A1 shRNA as a mock control. Besides of different transduction particles, control cells were treated similar.

After lentiviral transduction, a stable ALDH1A1 knockdown could be confirmed, based on western blot analysis 5 weeks and 2 months after transduction (s. Figure 4.1). In western blot analysis, a distinct difference of ALDH1A1 expression in ALDH1A1 knockdown cells (ADLH1A1-) and in the ALDH1A1 expressing control cell line (ALDH1A1+) can be seen, implying a successful ALDH1A1 knockdown in LN18 cells. Further Western Blot analysis also revealed stable knockdown after freezing and thawing cells (s. Figure 4.2).

In the following, LN18 cells with ALDH1A1 knockdown are labeled as ALDH1A1-, LN18 control cells, which express ALDH1A1 as ALDH1A1+.

Successful transducted cells were watched under the phase contrast microscope. No difference between ALDH1A1 knockdown cells (ALDH1A1-) and control cells (ALDH1A1+) in cell morphology could be observed (s. Figure 4.3).

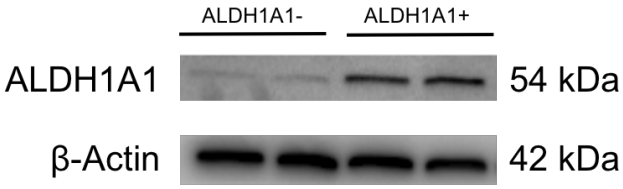

Figure 4.1 Western blot analysis 5 weeks after lentiviral transduction of LN18 cells. A distinct difference of ALDH1A1 expression in ALDH1A1+ and ALDH1A1- cells can be seen, implying a successful ALDH1A1 knockdown. Protein was analyzed by SDS-Page and Western blotting using monoclonal mouse anti-human ALDH1A antibody (Clone # 703410, R&D Systems Inc, 1:500) and monoclonal mouse anti-human β-Actin antibody (Clone AC-74, Sigma Aldrich, 1:2500) for loading control (s. 3.2.3). Molecular sizes of analyzed proteins are given on the right side. Anti-Mouse IgG (H+L) HRP conjugated antibodies (Sigma Aldrich) served as secondary antibodies. ALDH1A1+ = ALDH1A1 expressing control cells and ALDH1A1- = ALDH1A1 knockdown cells.

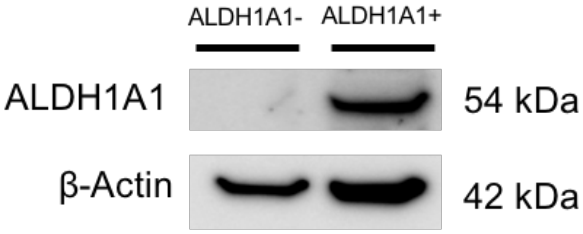

Figure 4.2 Western blot analysis: Confirmation of stable ALDH1A1 knockdown after freezing and thawing LN18 cells. Protein was analyzed by SDS-Page and Western blotting using monoclonal ALDH1A1 mouse antibody (Clone # 703410, R&D Systems Inc., 1:500) and monoclonal β-Actin mouse antibody (Clone AC-74, Sigma Aldrich) for loading control (s. 3.2.3). Molecular sizes of analyzed proteins are given on the right side. Anti-Mouse IgG (H+L) HRP conjugated antibodies (Sigma Aldrich) served as secondary antibodies. ALDH1A1+ = ALDH1A1 expressing control cells and ALDH1A1- = ALDH1A1 knockdown cells.

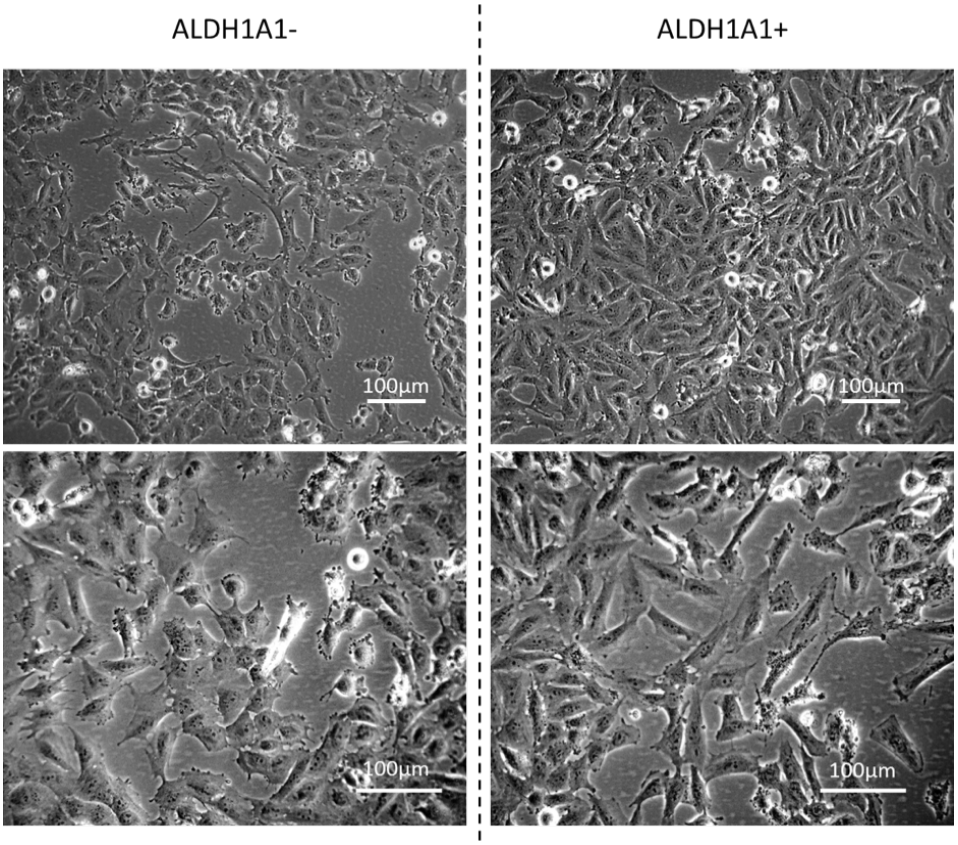

Figure 4.3 LN18 cells after lentiviral transduction with MISSION® Lentiviral Transduction Particles MISSION® Non-Mammalian shRNA Control Transduction Particles; Pictures show cells in passage 15 after incubation for 2 days under usual conditions under the phase contrast microscope. $5x10^5$ cells were seeded in a T75 cell culture flask. No difference in cell morphology between ALDH1A1 expressing cells ("ALDH1A1+") and ALDH1A1 knockdown cells ("ALDH1A1-") was observed.

4.2 ALDH1A1 knockdown has no influence on proliferation but plating efficiency

Alamarblue® proliferation assay with ALDH1A1+ and ALDH1A1- cells was performed over 96 h. Cell proliferation was measured using spectrophotometry. No differences in cell proliferation depending on ALDH1A1 expression could be seen (s. Figure 4.4).

Doubling time (DT) of both cell lines was determined assuming exponential cell growth. No significant differences in DT between ALDH1A1+ cells and ALDH1A1- could be observed. DT of ALDH1A1+ cells was ≈24 h ±3 h, DT of ALDH1A1- cells was ≈22 h ±1 h.

To measure the doubling time, different numbers of cells were seeded in triplicates (250, 500, 1000, 2000, 4000 cells per well). When seeded 500, 1000 and 2000 cells per well, growth curves showed exponential growth over the whole 96 h of observation, which suggested, that cells were in the log-phase of cell proliferation, in which doubling-time can be determined as accurately as possible. Therefore, doubling time was calculated from the mean of growth curves measured in wells with 500, 1000 and 2000 cells in the beginning.

In colony formation assay it was further found that plating efficiency (PE) of cell lines ALDH1A1+ and ALDH1A1- showed significant differences. ALDH1A1+ cells showed 1.5-fold higher PE than ALDH1A1- cells. (PE ALDH1A1+ ≈0.5 ±0.09; PE ALDH1A1- ≈0.3 ±0.05; $p<0.05$)

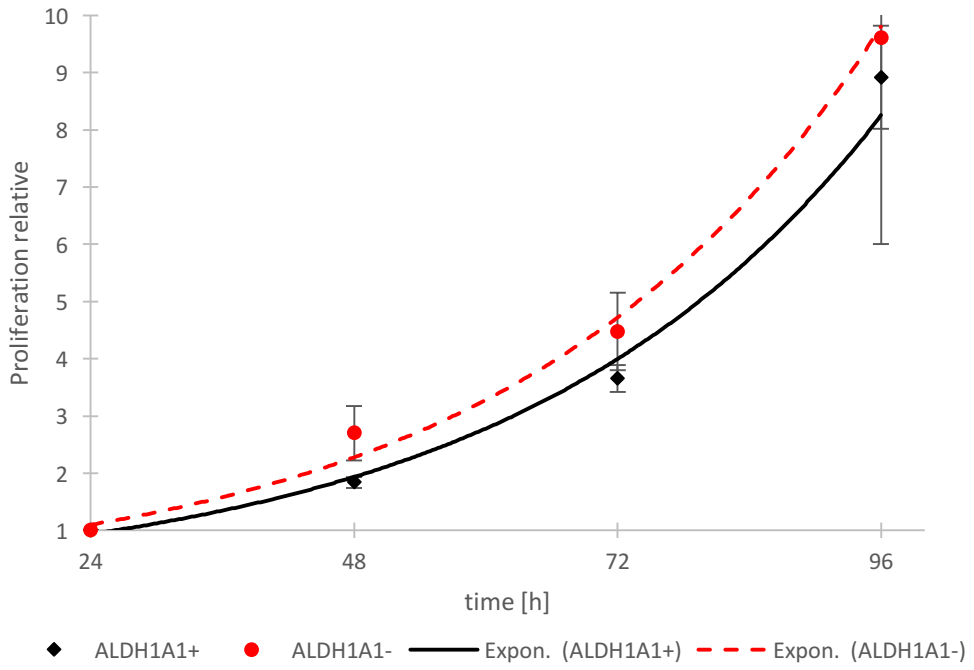

Figure 4.4 Alamar blue assay for proliferation analysis over 96 h of ALDH1A1+ and ALDH1A1- cells. Diagram shows proliferation curve when 500 cells per well were seeded. The relative proliferation was calculated based on the optical density (OD) of cells after 24 h in culture. There was no significant difference in proliferation between both cell lines. Data are shown as mean of 3 independent experiments. Error bars represent SEM.

4.3 ALDH1A1 knockdown leads to enhanced radiosensitivity

Colony formation assay was performed to compare colony formation of ALDH1A1+ cells with ALDH1A1- cells after X-ray-irradiation. ALDH1A1- formed significantly fewer colonies than ALDH1A1+ cells and hence had a much smaller survival fraction. Statistical analysis revealed highly significant differences in radioresistance between ALDH1A1+ and ALDH1A1- cells (s. Figure 4.5 and Figure 4.6).

Expressed in numbers, the dose which reduced surviving fraction (SF) of cells to 50%, the half maximal inhibitory dose (D_{50}), was 2.58 Gy for ALDH1A1+ cells compared to 1.91 Gy for ALDH1A1- cells. This means, that radiosensitivity in ALDH1A1- cells is 1.35-fold higher than in ALDH1A1+ cells. To kill 90% of the cell population (D_{10}), 6.21 Gy was necessary for ALDH1A1+ cells and 4.32 Gy for ALDH1A1- cells. This means even a 1.44-fold enhanced radiosensitivity in ALDH1A1- cells compared to ALDH1A1+ cells (s. Table 4.1).

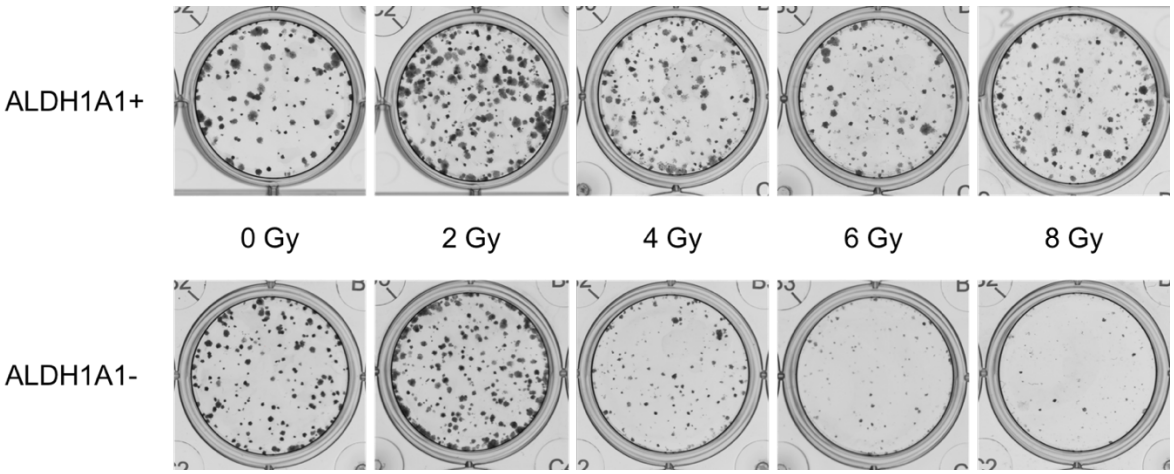

Figure 4.5 Colony formation assay; Single wells out of 12 well plates with ALDH1A1+ and ALDH1A1- cells, stained with crystal violet 12 days after irradiation. Pictures were taken with the GelCount™ colony counter.

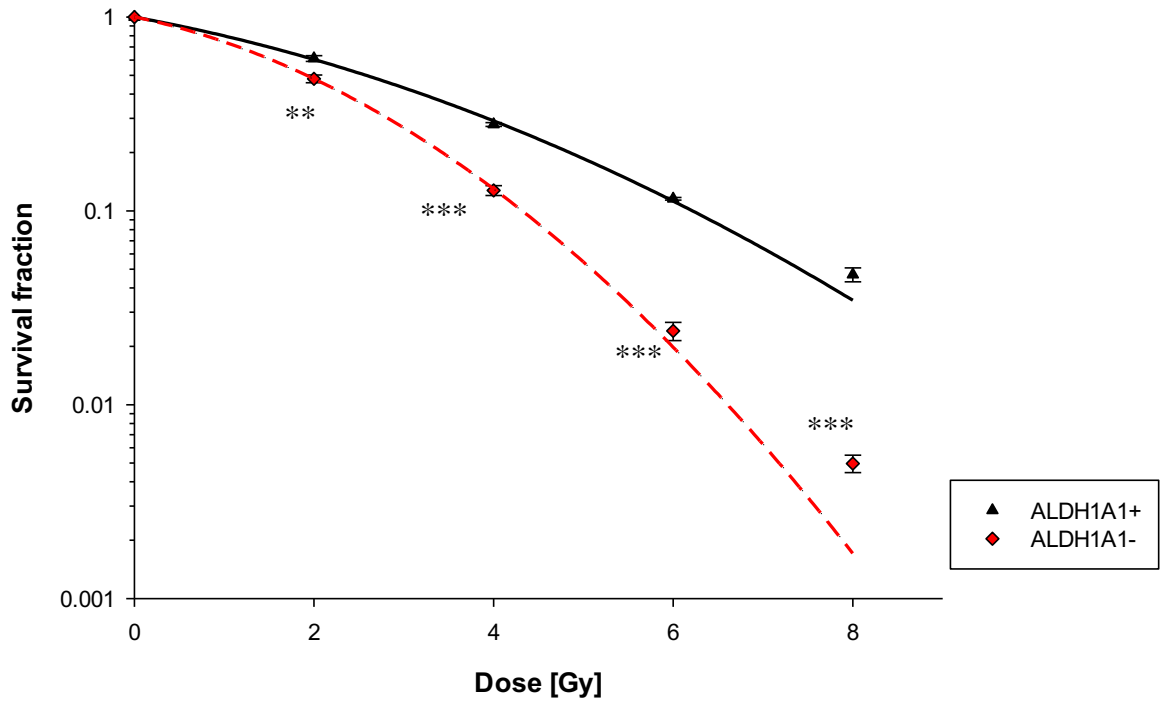

*Figure 4.6 Colony formation assay: logarithmic cell survival curves for cell lines ALDH1A1+ and ALDH1A1- after X-ray-irradiation with 0, 2, 4, 6 and 8 Gy. ALDH1A1- cells show significant lower survival after irradiation compared to ALDH1A1 expressing cell line ALDH1A1+. (**p<0.01; ***p<0.001). Data are shown as mean out of 4 independent experiments. Error bars represent SEM.*

Table 4.1 Summary of radiobiological parameters of ALDH1A1+ and ALDH1A1- cells.

	D_{50} [Gy]	SER (50%)	D_{10}	SER (10%)	α [Gy^{-1}]	β [Gy^{-2}]
ALDH1A1+	2.58	1	6.21	1	0.1961	0.0281
ALDH1A1-	1.91	**1.35**	4.32	**1.44**	0.2253	0.0714

Results of colony formation assay with α- and β-values derived from the linear quadratic model $SF = e^{-(\alpha D + \beta D^2)}$. D_{50} or D_{10} represent the irradiation doses [Gy] which are required to reduce the surviving fraction (SF) to 50% or 10%. Sensitizing enhancement ratio (SER) was calculated for SER (50%) with the formula [D_{50} ALDH1A1+ / D_{50} ALDH1A1-] and for SER (10%) with the formula [D_{10} ALDH1A1+ / D_{10} ALDH1A1-].

4.4 ALDH1A1 knockdown has no influence on cell cycle distribution after irradiation

Cell cycle analysis was done to investigate possible differences in cell cycle response to irradiation between ALDH1A1+ and ALDH1A1- cells. Cells were irradiated with 0, 4 and 8 Gy and fixed 24 h after irradiation. Flow cytometry analysis after PI (propidium iodide) staining revealed no major differences in cell cycle distribution between ALDH1A1+ and ALDH1A1- cells 24 h after irradiation (s. Figure 4.7 and Figure 4.8).

Significant accumulation of ALDH1A1+ and ALDH1A1- cells in G2/M phase and reduction of cells in G0/G1 phase depending on radiation dose could be observed (s. Figure 4.8).

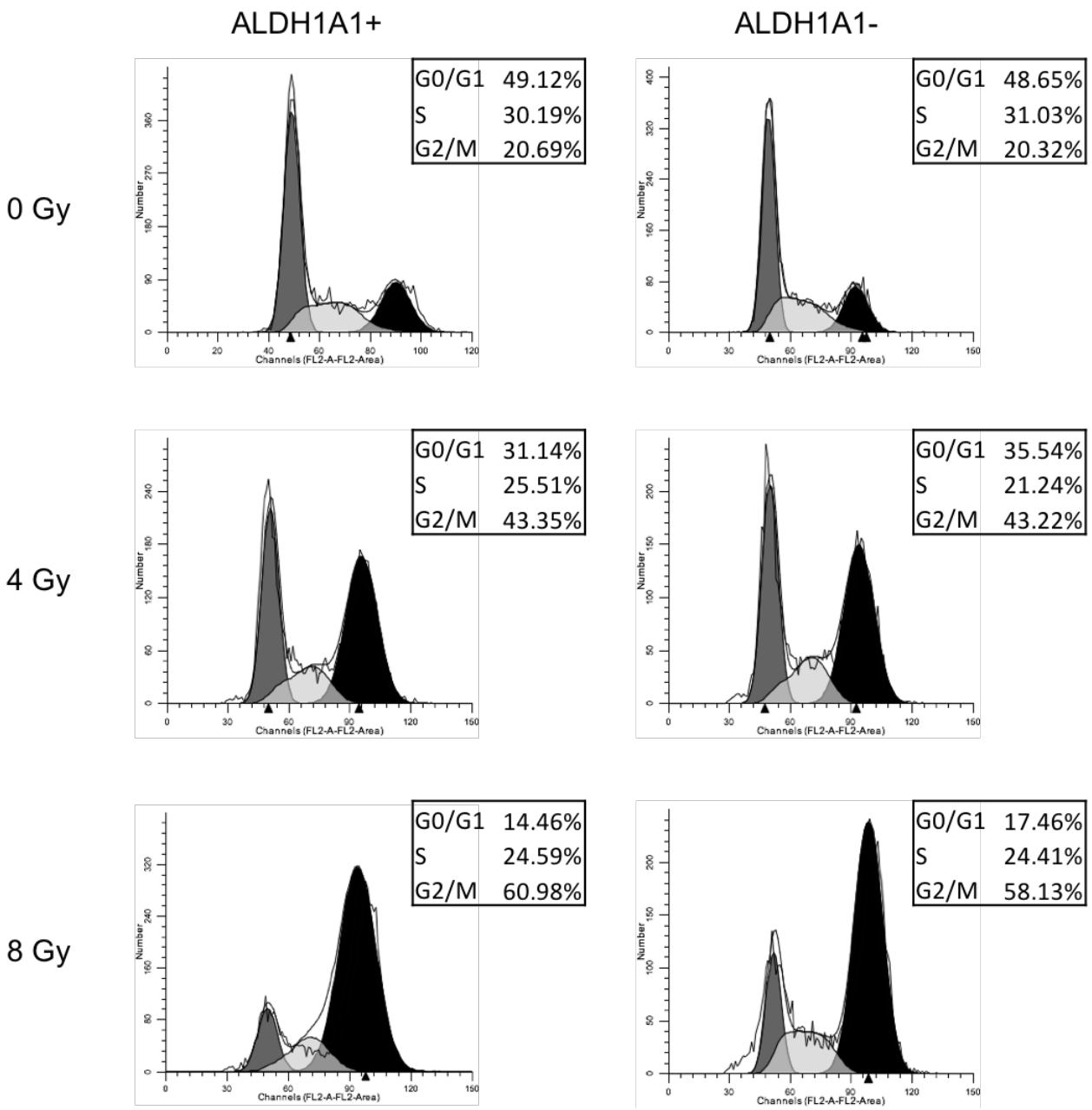

Figure 4.7 Representative FACS histograms of cell cycle distribution of ALDH1A1+ and ALDH1A1- cells 24 h after X-ray irradiation with 0, 4 and 8 Gy.

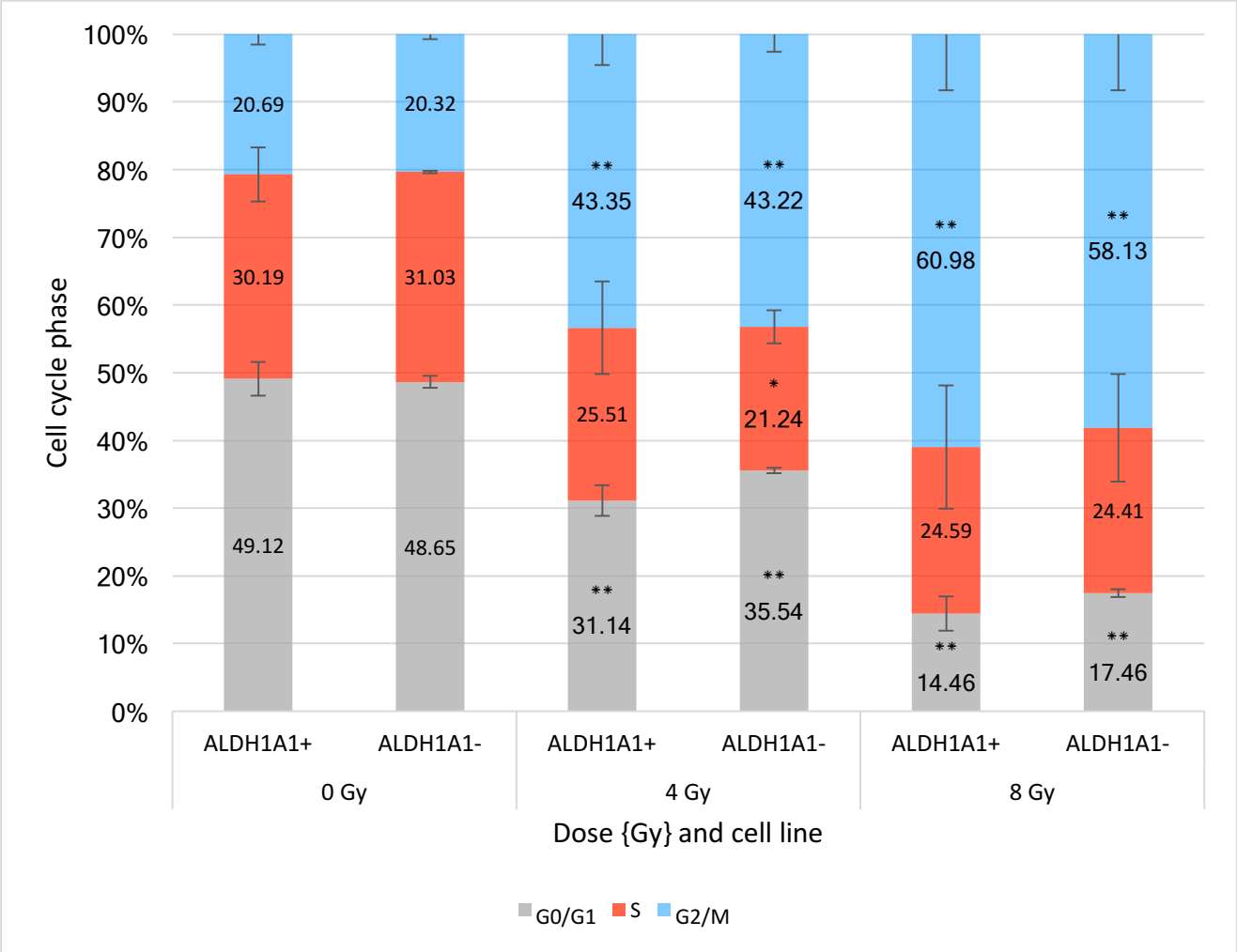

*Figure 4.8 Cell cycle distribution 24 h after irradiation. No significant differences in changes of cell cycle distribution 24 h after irradiation with 0, 4 and 8 Gy between ALDH1A1+ and ALDH1A1- cells could be observed. Significant changes of the cell cycle distribution between unirradiated and irradiated cells within one cell line are labeled with stars. (*p<0.05; **p<0.01).*

4.5 ALDH1A1 knockdown decreases migratory capacity in LN18 GBM cells

To determine whether the ADLH1A1 expression influences migratory capacity, wound healing assay was performed with ALDH1A1+ and ALDH1A1- cells (Fig. 4.9). To make sure that closing the cell free gap could not be due to cell proliferation, cells were kept in serum free medium (RPMI 1960 medium supplemented with 0.1% FBS).

Data from wound healing assay revealed significant differences in migratory capacity between ALDH1A1+ and ALDH1A1- cells. After 24 h ALDH1A1+ cells migrated 1.4-fold faster into the gap than ALDH1A1- cells (see Figure 4.10).

The difference in migratory capacity between ALDH1A1+ and ALDH1A1- cells was even greater when cells were irradiated with 8 Gy. Irradiated ALDH1A1+ GBM cells migrated 1.7-fold faster into the gap than ALDH1A1- cells. After 30 h a 1.5-fold higher relative migration could be observed (see Figure 4.11).

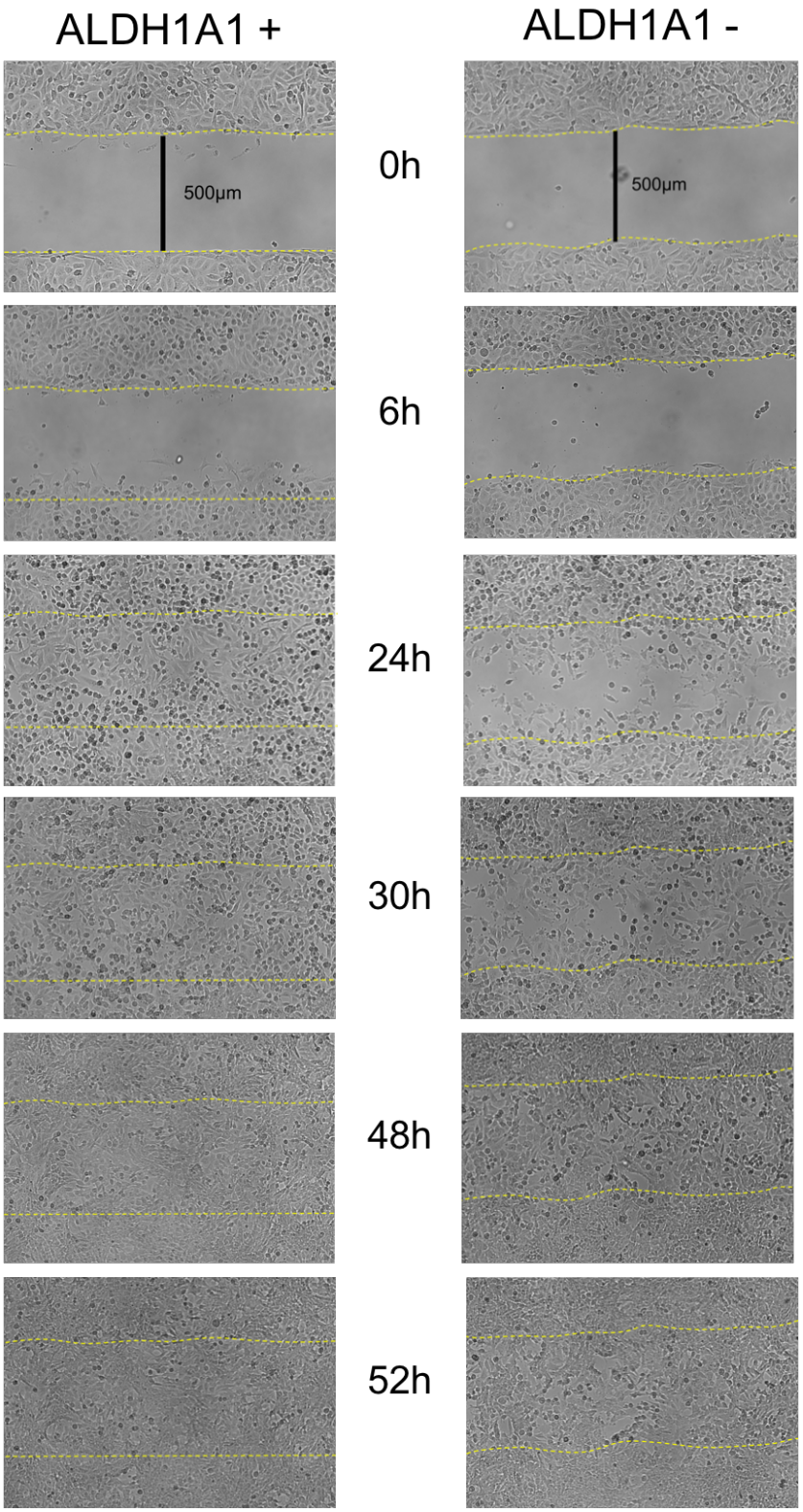

Figure 4.9 Pictures of wound healing assay taken under a bright-field microscope (10x magnification). These pictures show unirradiated ALDH1A1- and ALDH1A1+ cells migrating into the 500µm gap.

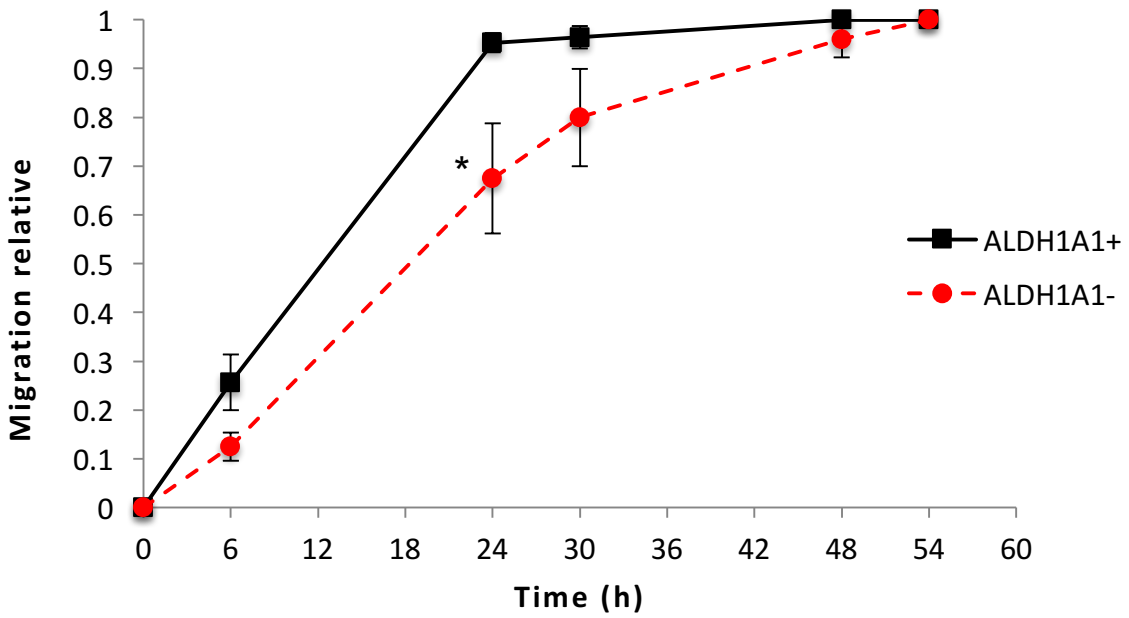

*Figure 4.10 Results of wound healing assays; Relative migration of ALDH1A1- cells and ALDH1A1+ cells. Significant differences in migration were seen after 24 h (*p<0.05). Time "0h" was defined by the time when culture-insert was removed from the well. Data are expressed as mean ± SEM (represented by error bars) out of 4 independent experiments.*

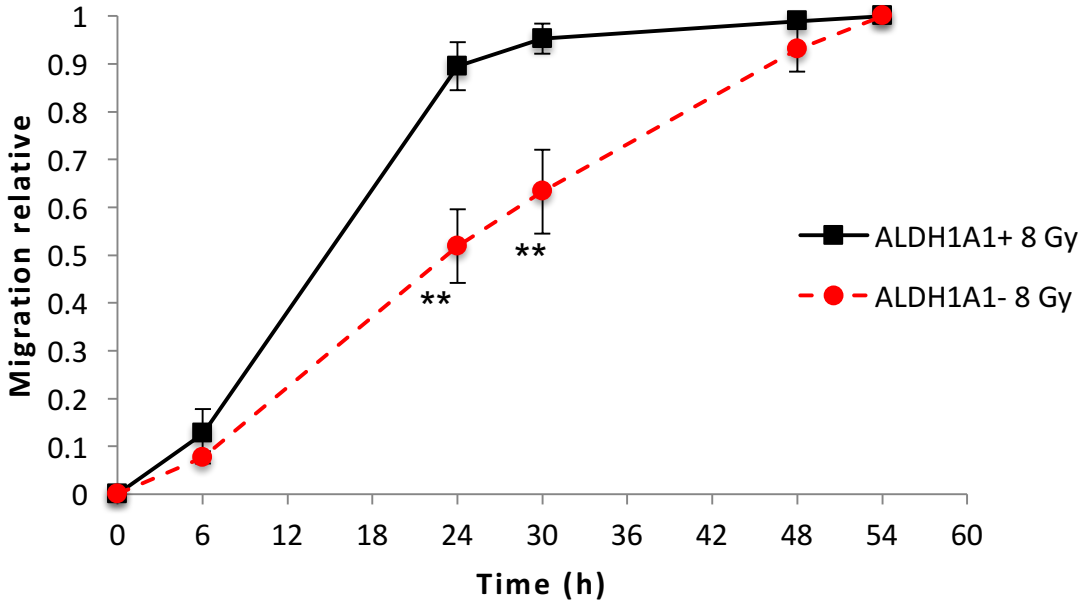

*Figure 4.11 Results of wound healing assays; Relative migration of ALDH1A1- cells and ALDH1A1+ cells after irradiation with 8Gy. Highly significant differences in migration were seen after 24 h and 30 h (**P<0.01). Time "0h" was defined by the time when culture-insert was removed from the well. Data are expressed as mean ± SEM (represented by error bars) out of 4 independent experiments.*

4.6 X-ray irradiation does not affect migration of ALDH1A1+ and ALDH1A1- LN18 GBM cells

To analyze whether X-ray-irradiation affects migratory behavior of ALDH1A1+ and ALDH1A1- cells, cells were irradiated with 0, 2 and 8 Gy prior to wound healing assay. Cells were irradiated in Ibidi® µ-dishes. First pictures for analysis of migratory capacity were taken immediately after irradiation (= time point 0 h). Serum free medium (RPMI 1960 medium supplemented with 0.1% FBS) was used to prevent biased results due to proliferation.

No significant differences in migration capacity between irradiated and non-irradiated cells could be seen for ALDH1A1+ as well as for ALDH1A1- cells at different time points (s. Figure 4.12 and Figure 4.13)

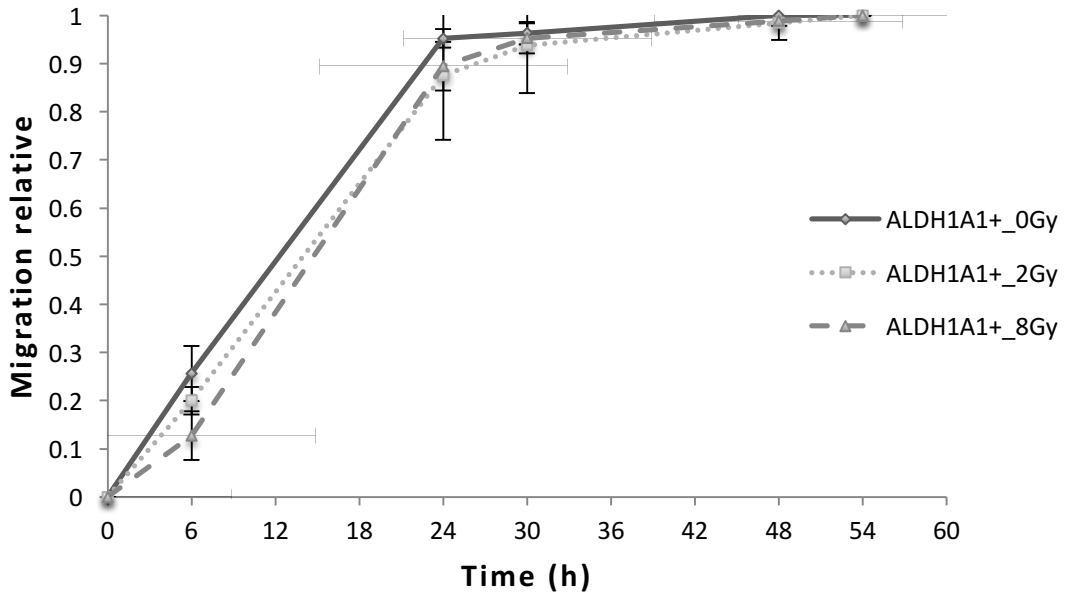

Figure 4.12 Migration of ALDH1A1+ cells after 0, 2 and 8 Gy. No significant differences in migratory capacity due to irradiation were seen. Time "0h" was defined by the time when culture-insert was removed from the well. Data are expressed as mean ± SEM (represented by error bars) out of 4 independent experiments.

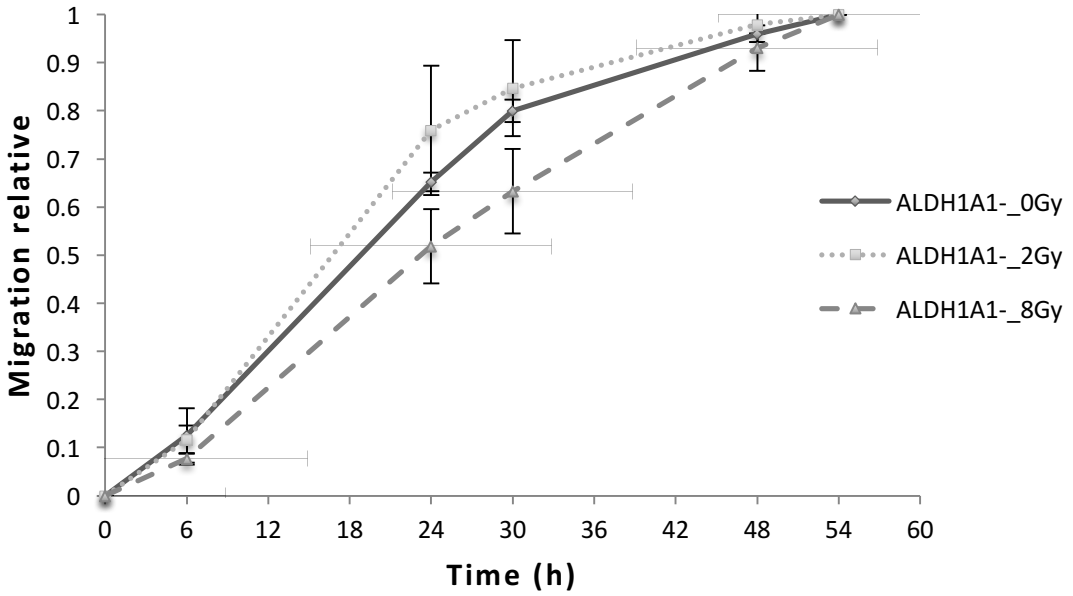

Figure 4.13 Migration of ALDH1A1- cells after 0, 2 and 8 Gy irradiation. No significant differences in migratory capacity due to irradiation were seen. Time "0h" was defined by the time when culture-insert was removed from the well. Data are expressed as mean ± SEM (represented by error bars) out of 4 independent experiments.

4.7 Hypoxia has no influence on ALDH1A1 expression

To answer the question, if hypoxia has an influence on ALDH1A1 expression in GBM cells, ALDH1A1+ and ALDH1A1- cells were exposed to hypoxic conditions (1% O_2) for 24 h and cell lysates for Western Blot analysis were prepared afterwards. ALDH1A1 expression was compared between cells which were incubated under hypoxia and cells which were incubated under normoxic conditions (21% O_2).

ALDH1A1+, as well as ALDH1A1- cells didn´t show any changes in ALDH1A1 expression after incubation under hypoxic conditions (s. Figure 4.14).

To prove that cells were exposed to hypoxia, the expression of the hypoxia-inducible protein carbonic anhydrase 9 (CA 9) was checked by western blot analysis. CA 9 was not detectable under normoxic conditions but strongly induced in ALDH1A1+ and ALDH1A1- cells that were exposed to hypoxic conditions.

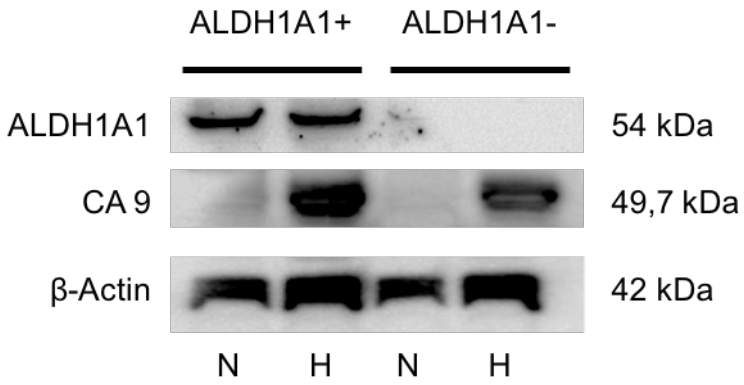

Figure 4.14 Western Blot analysis: ALDH1A1+ and ALDH1A1- cells after incubation under hypoxic conditions for 24 h (=H) compared to cells incubated under normoxic conditions (=N). Protein was analyzed by SDS-Page and Western blotting using monoclonal mouse anti-human ALDH1A antibody (Clone # 703410, R&D Systems Inc, 1:500), anti-human CA 9 antibody (Clone LS-B273, LifeSpan Bioscience, 1:1000) and monoclonal mouse anti-human β-Actin antibody (Clone AC-74, Sigma Aldrich, 1:2500) for loading control (s. 3.2.3). Molecular sizes of analyzed proteins are given on the right side. Anti-Mouse IgG (H+L) HRP conjugated antibodies (Sigma Aldrich) served as secondary antibodies. ALDH1A1+ = ALDH1A1 expressing control cells and ALDH1A1- = ALDH1A1 knockdown cells.

5 Discussion

GBM is one of the most malignant tumors and the most common primary brain tumor in adults. Despite extensive research in GBM treatment, no major improvements in therapy and patients´ prognosis have been made in the last years. Consequently, it is of highest clinical interest to find the reasons for GBM aggressiveness and thereby new targets for GBM treatment.

In recent years, ALDH1A1 was found to be a marker for cancer stem cells (CSCs) in GBM and several other solid tumor entities (Rasper et al. 2010, Meng et al. 2014, Yang et al. 2014). In addition, recent research has shown a correlation between ALDH1A1 expression and high aggressiveness of tumor cells. Most studies revealed an association between ALDH1A1 expression and poor clinical outcome for patients with clear cell renal cell carcinoma, breast cancer, esophageal squamous cell carcinoma and GBM (Campos et al. 2011, Wang et al. 2013, Liu et al. 2014, Yang et al. 2014). In contrast to that, Adam et al. stated, that ALDH1A1 is a marker of astrocytic differentiation during brain development and predicts better survival of GBM patients (Adam et al. 2012).

The role of ALDH1A1 for glioblastoma treatment still may appear of minor interest in relation to other great topics in GBM research. Nonetheless, Xu et al. observed ALDH1A1 expression in 34.2% of high-grade gliomas (WHO III-IV) compared to 8.5% in low-grade gliomas (WHO I-II) (Xu et al. 2015). In her doctoral thesis, Lämmer describes ALDH1A1 expression in 33.8% of patients with primary GBM and in 35.7% of patients with secondary GBM (Lämmer 2016). Adam et al. found ALDH1A1 expression even in 99% of tested primary GBMs in which the fraction of ALDH1A1 expressing tumor cells ranged from 0 to 49% (Adam et al. 2012). On top of that, Schäfer revealed enhanced ALDH1A1 expression in relapsed GBMs (Schäfer 2012). ALDH1A1 overexpression is expected to be correlated with high tumor aggressiveness, what has already been described above (Ginestier et al. 2007, Leinung et al. 2015). Therefore, it still seems to be appropriate to investigate the specific influence of ALDH1A1 expression on GBM cell properties. Focused analysis of ALDH1A1 function can provide interesting results not only for GBM but also for other tumor entities.

The aim of this study was to investigate, whether ALDH1A1 expression has an influence on GBM-cell-aggressiveness and radioresistance.

5.1 Stable ALDH1A1 knockdown in GBM cells – a proper model to investigate the function of ALDH1A1 in GBM?

The aim of this study was, to investigate, if ALDH1A1 expression in GBM cells has an influence on different tumor properties. To achieve this aim, an appropriate cell model was needed. For this reason, stable ALDH1A1 knockdown was successfully performed in GBM cell line LN18 using lentiviral transduction and RNA interference. Lentiviral transduction included generation of a mock transduced control cell line with steady ALDH1A1 expression.

This cell model can be regarded as a kind of an isogenic cell model. Compared to an isogenic cell model, gene expression was inhibited on mRNA level instead of DNA level and instead of parental wild-type cells, mock transduced cells were used as control cell line. With our model, like in isogenic cell models, the specific impact of the cellular genotype, in this case the expression of ALDH1A1, on the phenotype of GBM cells could be investigated.

In the following, the advantages, but also the limitations of our model are shortly reviewed.

One of the biggest advantages of our cell model was, that the stable ALDH1A1 knockdown in LN18 cells enabled us to investigate highly specific the impact of ALDH1A1 expression on distinct GBM properties such as radiosensitivity, migratory capacity and cell proliferation.

Compared with other technical possibilities to silence ALDH1A1 activity in cells, for example with pharmacological inhibition, there are no known side effects like inhibition or stimulation of other cellular mechanisms due to pharmacological interactions. Especially pharmacological inhibition may only block certain and not every function of ALDH1A1 and may also affect the function of other proteins of the ALDH superfamily. In contrast, RNA interference prevents gene expression at mRNA level and therefore inhibits every function of the ALDH1A1 very specifically.

The in vitro cell analysis also made it possible to observe cellular behavior without the influence of the tumor microenvironment or other influences beyond the cell itself.

At the same time, the lack of microenvironment in the model is one of the main limitations of this study, because microenvironment plays a pivotal role for tumor progression and behavior.

Furthermore, only one specific cell line was analyzed, which limits the general validity of the results. GBMs are very heterogeneous tumors consisting of highly heterogeneous cell populations. Thus, the cells used in this study aren´t representative for all GBM tumor cells or GBM CSCs.

5.2 ALDH1A1 expression and GBM cell proliferation

Proliferation of ALDH1A1+ and ALDH1A1- LN18 GBM cells was investigated using alamarBlue® proliferation assay. No differences in proliferation between the two cell lines could be observed. Thus, ALDH1A1 expression seems to have no influence on proliferation capacities of LN18 GBM cells.

ALDH1A1 is part of the Retinoic acid (RA) signaling pathway and therefore might play an important role in cell differentiation and proliferation (Marchitti et al. 2008). Thus, enhanced proliferation in ALDH1A1 high expressing cells compared with ALDH1A1 low expressing cells could be expected. However, reduced proliferation of GBM cells due to ALDH1A1 knockdown could not be observed in this study.

Our results are in contrast to a study by Xu et al., which showed increased proliferative capabilities in GBM cells with high ALDH1A1 expression (Xu et al. 2015). The conflicting results could be due to the

fact, that Xu et al. investigated ALDH1A1 dependent proliferation in cell lines which were sorted by Aldefluor® assay in ALDH high expressing and ALDH low expressing groups. This assay doesn´t allow a differentiation between the diverse ALDH-family members. Besides this, no further differences in these cells which could lead to enhanced or reduced proliferation capacities were analyzed. Based on the stable ALDH1A1 knockdown in our study, the only difference between the tested cell lines was ALDH1A1 expression. Therefore, the results of Xu et al. could be due to other mechanisms than ALDH1A1 expression or activity for example due to the activity of other enzymes of the ALDH family. Still, it must be mentioned, that Xu et al. also could show a significant correlation between ALDH1A1 overexpression and enhanced Ki-67 expression, a marker for proliferation, which is consistent with findings in other tumor entities, such as prostate cancer (Li et al. 2009) and pancreatic cancer (Kahlert et al. 2011). These studies also are in line with a work by Croker et al., who could show reduced proliferation in breast cancer cells after ALDH1A1 knockdown (Croker et al. 2017).

In contrast to that and in line with our findings, Adam et al. could not observe enhanced mitotic activity in ALDH1A1 expressing primary GBM cells (Adam et al. 2012). In this study, mitotic activity was shown in only 1.9% of ALDH1A1 expressing cells. Furthermore, no correlation between ALDH1A1 overexpression and enhanced proliferation could be found in HCC cancer cells (Tanaka et al. 2015). Considering that ALDH1A1 is regarded as marker for CSCs, which are slowly proliferating cells, it seems plausible that ALDH1A1 expressing cells might proliferate even less than ALDH1A1 non-expressing cells.

Consequently, the influence of ALDH1A1 expression on proliferation in tumor cells is discussed quite controversial in the literature. It seems, that ALDH1A1 expression has various impacts on proliferation in different tumor entities and cell lines.

Further investigation, e.g. proliferation analysis in ALDH1A1 overexpressing cells are needed to investigate the specific influence of ALDH1A1 expression on proliferation in tumor cells, especially in GBM cells.

5.3 ALDH1A1 expression and radioresistance in GBM cells

Radiotherapy is a cornerstone in GBM treatment. However, GBMs, especially recurrent GBMs, show enhanced radioresistance (Kelley et al. 2016). Several inherited or acquired cellular mechanisms as well as influences of the tumor microenvironment, which might be responsible for radioresistance in GBMs, have been investigated. Still, it is not fully understood, why GBMs are or become resistant towards radiotherapy.

ALDH1A1 is a marker for GBM progenitor cells (Rasper et al. 2010, Schäfer 2012) which are assumed to play a pivotal role for radioresistance of tumors (Mihatsch et al. 2011) as well as for GBM recurrence after first treatment (Dahan et al. 2014). Other research could show a correlation between high

ALDH1A1 expression, poor patient prognosis and enhanced tumor aggressiveness, including therapy resistance, in several tumor entities (Campos et al. 2011, Wang et al. 2013, Liu et al. 2014, Yang et al. 2014, Oria et al. 2018). For these reasons, we assumed that ALDH1A1 expression could affect or even cause resistance of GBM cells towards radiotherapy.

Colony formation assay (CFA), a well-established method to assess radiosensitivity of cells, revealed significantly higher radioresistance in ALDH1A1 expressing GBM cells compared to ALDH1A1 low expressing cells. The results are in line with a study by Cojoc et al., which revealed enhanced radioresistance in ALDH1A1 expressing prostate cancer cells (Cojoc et al. 2015).

Our study is the first one which could show a correlation between ALDH1A1 knockdown and increased radiosensitivity in GBM cells.

The reasons for enhanced radiosensitivity in GBM cells due to ALDH1A1 knockdown still need to be elucidated. Several possibilities, that could cause increased radioresistance of ALDH1A1 expressing GBM cells compared to ALDH1A1 knockdown cells can be discussed.

One possibility is, that enhanced ALDH1A1 expression and activity improve the effectiveness of detoxification of ROS induced toxic products. Ionizing radiation leads to ROS formation through radiolysis of water. Products of radiolysis such as hydroxyl radical ($^{\cdot}OH$), hydrogen peroxide (H_2O_2) and superoxide radical ($^{\cdot}O$-) can cause several cell damaging reactions, including lipid peroxidation, oxidation of amino acids within proteins and DNA and RNA damage (Azzam et al. 2012). Some studies could reveal, that cancer cells, especially CSCs show increased ROS scavenging pathways (Diehn et al. 2009, Shi et al. 2012, Chang et al. 2016). ALDH1A1 activity could be part of these scavenging pathways and thus lead to enhanced radioresistance. ROS mediated cell damages are in part due to ROS induced production of aldehydes. Enzymes of the ALDH1 family can detoxify aldehydes by oxidation. It was shown, that particularly ALDH1A1 is important for MDA (3,4-Methylenedioxyamphetamin) and 4-HNE (4-Hydroxynonenal) detoxification (Xiao et al. 2009, Kong and Kotraiah 2012). Furthermore, the role of ALDH1A1 activity in ROS detoxification has been shown by Lassen et al. in corneal and lens cells of mice. In these cells, ALDH1A1 was found to protect the tissue from UV irradiation induced ROS mediated damage (Lassen et al. 2007). Therefore, our finding, that ALDH1A1 expression in GBM cells enhanced radioresistance could be due to the role of ALDH1A1 in ROS scavenging pathways.

Enhanced G2/M checkpoint control and upregulation of DNA damage response (DDR) have been discussed to be responsible for radioresistance of CSCs (Ropolo et al. 2009, Carruthers et al. 2015). As ALDH1A1 is a marker for GBM stem cells, another mechanism, which could lead to enhanced radioresistance in ALDH1A1 expressing cells is enhanced G2/M checkpoint control and upregulation of DNA damage response (DDR).

However, cell cycle analysis of ALDH1A1+ and ALDH1A1- cells 24 h after X-ray irradiation with 4 and 8 Gy did not show any differences in cell cycle distribution between the two cell lines. The results lead

to the assumption, that enhanced radioresistance in ALDH1A1 expressing cells is not due to enhanced G2/M checkpoint activation.

Further experiments, not only in the GBM cell line LN18, such as γ-H2AX-assay, single cell gel electrophoresis or cell cycle analysis at different time points of ALDH1A1+ and ALDH1A1- GBM cells, should be performed to allow more accurate statements about enhanced radioresistance in ALDH1A1 expressing GBM cells and the underlying mechanisms.

5.4 The impact of ALDH1A1 expression on migration of GBM cells

This study revealed significant higher migratory capacity of ALDH1A1+ LN18 GBM cells compared to ALDH1A1- LN18 GBM cells. Migration was investigated by the well-established wound healing assay, using serum free medium to prevent wound closure due to cell proliferation.

Our observations go in line with recent research demonstrating enhanced migratory capacities in ALDH1A1 expressing cells in esophageal squamous cell carcinoma (Yang et al. 2014), in HCC (Yan et al. 2016) and in GBM (Xu et al. 2015).

It is not completely understood, why ALDH1A1 expressing cells show enhanced cell motility and migratory capacities. ALDH1A1 was found to be involved in detoxification of aldehydes as well as in RA signaling. These functions seem to have no influence on cell motility or cell migration. Different possibilities and mechanisms, how ALDH1A1 could have a direct influence on cell migration are discussed in the literature. Yan et al. could show increased cell motility in ALDH1A1 expressing HCC cancer cells. Enhanced migration of ALDH1A1 expressing HCC cells was due to the function of ALDH1A1 as a Gli2 stabilizing factor which is involved in the Hedgehog (Hh) signaling pathway (Yan et al. 2016). Chang et al. revealed the impact of aberrant Hh signaling on cell migration in GBM cells (Chang et al. 2015). Taken together, these studies indicate, that ALDH1A1 does not only function as an enzyme, but also as a protein-stabilizing factor and therefore affects signaling pathways (e.g. Hh) within tumor cells, which might lead to enhanced migratory capacity.

A study by Yang et al. reported enhanced migration and invasion in ALDH1A1 high expressing esophageal squamous cell carcinoma cells (Yang et al. 2014). In this study Yang et al. recognized a strong correlation between ALDH1A1 expression and the expression of MMPs and vimentin. Furthermore, there was a correlation between high levels of ALDH1A1 and decreased expression of E-cadherin. This leads to the assumption, that ALDH1A1 expression is associated with epithelial-mesenchymal transition (EMT).

In 2014 Meng et al. reported on a gene signature comprising 31 genes in GBM cells which could serve as a predictive marker especially for outcome after radiotherapy (Meng et al. 2014). In the same study, Meng et al. could show that enhanced epithelial mesenchymal transition (EMT) was associated with a

radioresistant phenotype in GBM cells. ALDH1A1 might be regulated by one of these genes and therefore lead to enhanced migratory capacity due to EMT and radioresistance.

Apart from that, ALDH1A1 was found to be a CSC marker in several tumor entities. It was shown by several studies, that CSCs have enhanced migratory capacity. Munthe et al. revealed, that migrating glioma cells could regrow tumors and therefore might be responsible for tumor relapse (Munthe et al. 2016). GBM relapses occur mostly in the region 2-3 cm close to the primary tumor (Loeffler et al. 1990). In this context, it is of highest interest, that the largest numbers of ALDH1A1 overexpressing cells were found in the tumor adjacent regions of GBMs (Xu et al. 2015, Lämmer 2016).

Most of the studies mentioned above observed enhanced ALDH1A1 expression in tumor cells associated with the concomitant expression of CSC properties. This suggests, that ALDH1A1, as a common CSC marker, is a marker for enhanced migration and invasion. In our model, cells differ only in ALDH1A1 expression. Our results indicate, that ALDH1A1 is not only associated with enhanced migratory capacities but might even cause migration in GBM cells. More detailed investigations are needed to elucidate the underlying mechanisms.

5.4.1 Influence of irradiation on migration in GBM

Enhanced migration of GBM cells after X-ray irradiation has been described in the literature before (Wild-Bode et al. 2001, Zhai et al. 2006, Rieken et al. 2011, Shankar et al. 2014). Therefore, we compared migratory capacity of ALDH1A1+ and ALDH1A1- LN18 cells after treatment with 0, 2 and 8 Gy irradiation. In contrast to the literature mentioned above we could not observe any differences in migratory capacity of ALDH1A1+ as well as ALDH1A1- LN18 GBM cells after irradiation with 0, 2 and 8 Gy.

To see our results in the right context with other research, it must be said, that the experimental settings in the literature mentioned above differ from the ones in our study.

We investigated migration using wound healing assay, a well-established and often used assay to investigate 2D migration *in vitro*. Migration was examined after irradiation in only two cell lines. Time of irradiation prior to observation of migration was not varied. To give an example, Rieken et al. (Rieken et al. 2011) started migration assay 24 h after irradiation. It is conceivable, that changes within the tumor cells after irradiation, which could lead to enhanced migration, need time to occur.

Shankar et al. (Shankar et al. 2014) observed enhanced migration in GBMs in an *in vivo* rat model after subcurative irradiation. In our *in vitro* study, the well-established GBM cell line LN18 was irradiated with exactly defined doses under usual cell culture conditions. Therefore, it is difficult to compare our results with the ones from Shankar et al.

In conclusion, further experiments with distinct ALDH1A1 expressing GBM cell lines, different doses and types of irradiation and different migration assays need to be performed to investigate migration after irradiation in GBMs in greater detail.

5.5 Evaluation of the influence of hypoxia on ALDH1A1 expression

In GBMs, regions with insufficient blood supply and therefore reduced oxygen levels are seen frequently. Growing evidence exists about the role of hypoxia in maintaining stem cell properties such as self-renewal and pluripotent differentiation capacity. Still, the underlying mechanisms are not fully understood yet. Furthermore, hypoxic niches within tumors are discussed to harbor CSCs, protecting these cells against chemo- and radiotherapy (Heddleston et al. 2009, Filatova et al. 2013, Inukai et al. 2015).

Hypoxia enhances ROS production and therefore can lead to cell damaging ROS levels within the cell. Considered that ALDH1A1 plays a role in detoxification of ROS, it stands to reason, that ALDH1A1 expression is up-regulated by hypoxia. Reduction of ROS levels due to hypoxia induced ALDH1A1 upregulation could prevent ROS induced cell damage and lead to low ROS levels within cancer cells.

Furthermore, ALDH1A1 is a marker for GBM progenitor cells. Therefore, one of the research questions of this study was, if hypoxia induces ALDH1A1 expression in GBM cells. In the present experiments, no influence of hypoxia on ALDH1A1 expression in ALDH1A1+ and ALDH1A1- cells could be observed.

This stands in contrast to what Soehngen et al. described in 2014 (Soehngen et al. 2014). He observed enhanced ALDH1 expression and increased neurosphere formation in ALDH1 expressing GBM cells following incubation under hypoxic cell culturing conditions for 24 h. Soehngen et al. therefore deduces that ALDH1 is a marker for tumor-initiating cells and that hypoxic microenvironment in GBM could lead to dedifferentiation of tumor cells towards CSCs. Of note, Soehngen et al. only investigated ALDH1 expression and not the expression of the ALDH family member ALDH1A1. The ALDH1 family includes 3 enzymes, ALDH1A1, ALDH1A2 and ALDH1A3. Thus, enhanced ALDH1 expression in his study could be due to enhanced expression of another ALDH1 family member.

5.6 ALDH1A1 as a new prognostic marker and therapy target in GBM

In the last decades, only small advances have been made in GBM treatment and treatment prognostics. Therefore, new therapy targets and prognostic markers for GBM patients are desperately needed. Based on the results of this study, ALDH1A1 could serve as a new prognostic marker and therapy target in GBM.

Deduced from the results of this study, ALDH1A1 is a marker for enhanced radioresistance and increased migratory capacity and therefore might predict a worse clinical outcome in patients. At the same time, patients with high ALDH1A1 could profit from new therapies targeting ALDH1A1. Lämmer

et al. could detect ALDH1A1 expression in 33.8 % of patients with primary GBM and in 35.7% of patients with secondary GBM (Lämmer 2016). For these patients, inhibition of ALDH1A1 could sensitize GBM cells towards radiotherapy and might help to overcome radioresistance of normal GBM cells but also GCSCs.

In the last years, it has become more and more apparent, that for successful GBM treatment, CSCs within tumors need to be eradicated. CSCs are considered being responsible for tumor progression, relapse and therapy resistance. As described above, Xu et al. revealed enhanced ALDH1A1 expression in GBM cells located at the tumor margins (Xu et al. 2015). Recurrent GBMs usually occur in the region 2-3 cm from the primary tumor bed (Loeffler et al. 1990).

Furthermore, there is much evidence, that ALDH1A1 activity induces chemoresistance, especially resistance against the alkylating agent temozolomide (TMZ) (Schäfer et al. 2012). As was shown by Rasper et al. ALDH1A1 is a marker for GBM progenitor cells that means, that ALDH1A1 expressing cells are able to regrow tumors (Rasper et al. 2010).

Connected with our results it is thinkable, that ALDH1A1 expressing cells might escape radiotherapy, due to enhanced radioresistance and migration and lead to tumor relapse.

Studies must show if it is possible to inhibit ALDH1A1 activity *in vivo.* Different kinds of ALDH1A1 inhibitors have been investigated in the last years. Several substances such as DEAB (N,N-diethylaminobenzaldehyde) and Disulfiram are able to inhibit ALDH1A1 efficient (Koppaka et al. 2012). Still, future clinical studies have to, prove whether these substances can be safely used in GBM treatment and most important, if treatment with ALDH1A1 inhibitors has a favorable effect on patients´ prognosis.

6 Summary and Outlook

Glioblastoma multiforme (GBM) is the most common primary brain tumor in adults with a devastating prognosis with a median survival of 15 months. Despite multimodal therapy, including surgery, chemotherapy and radiotherapy, GBM recurrence after first treatment is nearly inevitable. GBM aggressiveness and relapse is due to the aggressive character of GBM tumor cells and therapy resistance. In the last decades, research could not improve patients´ prognosis more than a few months. Approaches in GBM diagnosis and treatment are desperately needed.

ALDH1A1, a cytosolic enzyme belonging to the ALDH enzyme superfamily, was shown to be a marker for cancer stem cells (CSCs) in several solid tumor entities including GBM (Rasper et al. 2010). Xu et al. could show a correlation between ALDH1A1 expression in GBM cells and enhanced aggressiveness and dismal prognosis (Xu et al. 2015).

Thanks to the successful establishment of a stable ALDH1A1 knockdown in GBM LN18 cells by lentiviral transduction, we could show for the first time, that ALDH1A1 expression in GBM cells significantly enhances radioresistance, one of the main problems in GBM treatment. Cell cycle analysis did not reveal any differences in cell cycle distribution of ALDH1A1+ and ALDH1A1- cell lines after X-ray irradiation. Therefore, the mechanisms leading to enhanced radioresistance due to ALDH1A1 expression stay nebulous.

Furthermore, increased migratory capabilities of ALDH1A1 expressing GBM cells compared to ALDH1A1 knockdown cells could be seen in wound healing assay. Differences were even more significant after irradiating cells with 8 Gy before performing wound healing assay.

Existing research, which showed enhanced proliferation in ALDH1A1 high expressing cells compared to ALDH1A1 low expressing cells could not be confirmed in the present investigation. Moreover, no influence of hypoxia on ALDH1A1 levels in GBM cells, what was described by Soehngen et al. (Soehngen et al. 2014) could be observed. Also, there was no increased migration of GBM cells after irradiation, as was seen by Wild-Bode et al. (Wild-Bode et al. 2001) and Rieken et al. (Rieken et al. 2011), neither in ALDH1A1+ nor in ALDH1A1- LN18 cells.

Due to our results, ALDH1A1 could serve as a new prognostic marker for GBM patients, indicating high aggressiveness and radioresistance. Furthermore, targeting ALDH1A1 could be a novel strategy to eradicate GBM CSCs and to overcome radioresistance, even in the ALDH1A1 expressing cell population within GBMs as well as in other ALDH1A1 expressing tumor entities.

7 Danksagung

Hiermit möchte ich mich herzlich bei Frau Dr. Daniela Schilling bedanken, die viel Zeit, organisatorische Arbeit und vor allem Hirn in mich und meine Arbeit investiert hat und die für mich jederzeit hilfsbereit ansprechbar war!

Auch möchte ich mich für die Betreuung und für die ursprüngliche Idee zu dieser Arbeit bei Frau Prof. Dr. Stephanie Combs und Herrn PD Dr. Thomas Schmid bedanken.

Außerdem danke ich Frau Dr. Friederike Lämmer und Michaela Wank für ihren fachlichen Input, der für meine Arbeit sehr hilfreich und v.a. nötig war.

Ein weiterer großer Dank geht an den hoch kompetenten, fleißigen und immer für gute Stimmung im Labor zu habenden MTA Marlon Stein. Ohne ihn hätte die ein oder andere Zellkultur meine Kurzurlaube oder Prüfungsphasen nicht überstanden. Genauso, wie ich viele lange Mittags- und Blotting-Pausen nicht überstanden hätte, ohne Frau Dr. Sofie Dobiasch, der ich für die „seelisch-moralische“ Unterstützung meiner Doktorarbeit danken möchte.

Zuletzt möchte ich meinen Eltern Dr. med. Ulrike und Dr. med. Helmut Martin danken, dafür, dass Sie mich bei meiner Doktorarbeit genauso wie bei allen anderen meiner „Aktivitäten“ voll und ganz unterstützt haben. Wie man aus ihren Titeln eventuell ableiten könnte, haben sie mich womöglich seit meiner frühen Kindheit dazu „inspiriert“ irgendwann selbst einen solchen Titel im Namen tragen zu wollen... Doch nicht nur seelische Unterstützung und Inspiration haben meine Eltern zu dieser Arbeit beigetragen. Sie haben es überhaupt erst möglich gemacht, dass ich Semesterferien, freie Nachmittage und Wochenenden im Labor und nicht bei einer geldeinbringenden Tätigkeit verbracht habe, sie sind also mit die wichtigsten „Sponsoren“ dieser Arbeit. Vielen, vielen Dank dafür!

Figures

Figure 1.1 Genetic pathways to primary and secondary GBM and their clinical differences modified from (Ohgaki et al. 2004, Ohgaki and Kleihues 2013). (EGFR, epithelial growth factor receptor IDH1, isocitrate dehydrogenase 1; LOH, loss of heterozygosity; p16ink4a, cyclin-dependent kinase inhibitor 2A; PTEN, phosphatase and tensin homolog; TP53, tumor protein p53; MST, mean survival time). 2
Figure 1.2 Cancer stem cell theory – Hierarchical model: Cells within tumors can be hierarchically organized, ranging from highly differentiated, less proliferative cells to almost undifferentiated, highly proliferative cells. 4
Figure 1.3 Stochastic model of tumorigenesis 5
Figure 1.4 Glioblastoma multiforme in the right frontotemporal lobe. Thankfully obtained by Dr. med. Christoph Straube, Department of Radiation Oncology, Technical University of Munich (TUM), Germany. 6
Figure 1.5 Mechanisms of radioresistance in GBM cancer stem cells (GCSCs) modified from (Kelley et al. 2016). (ROS, reactive oxygen species; Wnt, “Wingless/Integrated”; SHH, sonic hedgehog). 8
Figure 1.6 The reaction catalyzed by ALDH. Aldehydes get oxidized to their corresponding carboxylic acid. 9
Figure 1.7 The function of ALDHs (aldehyde dehydrogenase) in CSCs (cancer stem cells) (Duester 2000, Vasiliou and Nebert 2005, Xu et al. 2015) 10
Figure 3.1 Schematic overview of the intracellular processes due to lentiviral transduction. 19
Figure 3.2 TRC1 and TRC1.5 Lentiviral Plasmid Vector pLKO.1-puro Features. Source: Sigma-Aldrich, Inc., St. Louis, USA. 20
Figure 3.3 Schematic structure of tank blot system for protein transfer from gel to PVDF membrane 23
Figure 3.4 Chemical reaction of alamarBlue®. Resazurin, which is non-fluorescent, is converted to redfluorescent Resafurin due to cells´metabolism. 26
Figure 4.1 Western blot analysis 5 weeks after lentiviral transduction of LN18 cells. A distinct difference of ALDH1A1 expression in ALDH1A1+ and ALDH1A1- cells can be seen, implying a successful ALDH1A1 knockdown. Protein was analyzed by SDS-Page and Western blotting using monoclonal mouse anti-human ALDH1A antibody (Clone # 703410, R&D Systems Inc, 1:500) and monoclonal mouse anti-human β-Actin antibody (Clone AC-74, Sigma Aldrich, 1:2500) for loading control (s. 3.3.4). Molecular sizes of analyzed proteins are given on the right side. Anti-Mouse IgG (H+L) HRP conjugated antibodies (Sigma Aldrich) served as secondary antibodies. ALDH1A1+ = ALDH1A1 expressing control cells and ALDH1A1- = ALDH1A1 knockdown cells. 30
Figure 4.2 Western blot analysis: Confirmation of stable ALDH1A1 knockdown after freezing and thawing LN18 cells. Protein was analyzed by SDS-Page and Western blotting using monoclonal ALDH1A1 mouse antibody (Clone # 703410, R&D Systems Inc., 1:500) and monoclonal β-Actin mouse antibody (Clone AC-74, Sigma Aldrich) for loading control (s. 3.3.4). Molecular sizes of

analyzed proteins are given on the right side. Anti-Mouse IgG (H+L) HRP conjugated antibodies (Sigma Aldrich) served as secondary antibodies. ALDH1A1+ = ALDH1A1 expressing control cells and ALDH1A1- = ALDH1A1 knockdown cells. 30

Figure 4.3 LN18 cells after lentiviral transduction with MISSION® Lentiviral Transduction Particles MISSION® Non-Mammalian shRNA Control Transduction Particles; Pictures show cells in passage 15 after incubation for 2 days under usual conditions under the phase contrast microscope. $5x10^5$ cells were seeded in a T75 cell culture flask. No difference in cell morphology between ALDH1A1 expressing cells ("ALDH1A1+") and ALDH1A1 knockdown cells ("ALDH1A1-") was observed. 31

Figure 4.4 Alamar blue assay for proliferation analysis over 96 h of ALDH1A1+ and ALDH1A1- cells. Diagram shows proliferation curve when 500 cells per well were seeded. The relative proliferation was calculated based on the optical density (OD) of cells after 24 h in culture. There was no significant difference in proliferation between both cell lines. Data are shown as mean of 3 independent experiments. Error bars represent SEM. 32

Figure 4.5 Colony formation assay; Single wells out of 12 well plates with ALDH1A1+ and ALDH1A1- cells, stained with crystal violet 12 days after irradiation. Pictures were taken with the GelCount™ colony counter. 33

Figure 4.6 Colony formation assay: logarithmic cell survival curves for cell lines ALDH1A1+ and ALDH1A1- after X-ray-irradiation with 0, 2, 4, 6 and 8 Gy. ALDH1A1- cells show significant lower survival after irradiation compared to ALDH1A1 expressing cell line ALDH1A1+. (**p<0.01; ***p<0.001). Data are shown as mean out of 4 independent experiments. Error bars represent SEM. 34

Figure 4.7 Representative FACS histograms of cell cycle distribution of ALDH1A1+ and ALDH1A1- cells 24 h after X-ray irradiation with 0, 4 and 8 Gy. 36

Figure 4.8 Cell cycle distribution 24 h after irradiation. No significant differences in changes of cell cycle distribution 24 h after irradiation with 0, 4 and 8 Gy between ALDH1A1+ and ALDH1A1- cells could be observed. Significant changes of the cell cycle distribution between unirradiated and irradiated cells within one cell line are labeled with stars. (*p<0.05; **p<0.01). 37

Figure 4.9 Pictures of wound healing assay taken under a bright-field microscope (10x magnification). These pictures show unirradiated ALDH1A1- and ALDH1A1+ cells migrating into the 500µm gap. 39

Figure 4.10 Results of wound healing assays; Relative migration of ALDH1A1- cells and ALDH1A1+ cells. Significant differences in migration were seen after 24 h (*p<0.05). Time "0h" was defined by the time when culture-insert was removed from the well. Data are expressed as mean ± SEM (represented by error bars) out of 4 independent experiments. 40

Figure 4.11 Results of wound healing assays; Relative migration of ALDH1A1- cells and ALDH1A1+ cells after irradiation with 8Gy. Highly significant differences in migration were seen after 24 h and 30 h (**P<0.01). Time "0h" was defined by the time when culture-insert was removed from the well. Data are expressed

as mean ± SEM (represented by error bars) out of 4 independent experiments. 40
Figure 4.12 Migration of ALDH1A1+ cells after 0, 2 and 8 Gy. No significant differences in migratory capacity due to irradiation were seen. Time “0h” was defined by the time when culture-insert was removed from the well. Data are expressed as mean ± SEM (represented by error bars) out of 4 independent experiments.41
Figure 4.13 Migration of ALDH1A1- cells after 0, 2 and 8 Gy irradiation. No significant differences in migratory capacity due to irradiation were seen. Time “0h” was defined by the time when culture-insert was removed from the well. Data are expressed as mean ± SEM (represented by error bars) out of 4 independent experiments. 42
Figure 4.14 Western Blot analysis: ALDH1A1+ and ALDH1A1- cells after incubation under hypoxic conditions for 24 h (=H) compared to cells incubated under normoxic conditions (=N). Protein was analyzed by SDS-Page and Western blotting using monoclonal mouse anti-human ALDH1A antibody (Clone # 703410, R&D Systems Inc, 1:500), anti-human CA 9 antibody (Clone LS-B273, LifeSpan Bioscience, 1:1000) and monoclonal mouse anti-human β-Actin antibody (Clone AC-74, Sigma Aldrich, 1:2500) for loading control (s. 3.3.4). Molecular sizes of analyzed proteins are given on the right side. Anti-Mouse IgG (H+L) HRP conjugated antibodies (Sigma Aldrich) served as secondary antibodies. ALDH1A1+ = ALDH1A1 expressing control cells and ALDH1A1- = ALDH1A1 knockdown cells. 43

Tables

Table 1.1 GBM subtypes: Genetic and clinical characteristics (Verhaak et al. 2010) 2
Table 3.1 Technical devices 13
Table 3.2 Software 14
Table 3.3 Chemicals and reagents 14
Table 3.4 Consumables 17
Table 3.5 Buffers and solutions 21
Table 3.6 Gel preparation for SDS-Page 22
Table 3.7 Antibodies 24
Table 3.8 Seeded cell numbers for CFA 25
Table 3.9 Propidium iodide staining solution 27
Table 4.1 Summary of radiobiological parameters of ALDH1A1+ and ALDH1A1- cells. 34

References

Adam, S. A., O. Schnell, J. Pöschl, S. Eigenbrod, H. A. Kretzschmar, J.-C. Tonn and U. Schüller (2012). "ALDH1A1 is a Marker of Astrocytic Differentiation during Brain Development and Correlates with Better Survival in Glioblastoma Patients." Brain Pathology **22**(6): 788-797.

Al-Hajj, M., M. S. Wicha, A. Benito-Hernandez, S. J. Morrison and M. F. Clarke (2003). "Prospective identification of tumorigenic breast cancer cells." Proceedings of the National Academy of Sciences of the United States of America **100**(7): 3983-3988.

Anido, J., A. Saez-Borderias, A. Gonzalez-Junca, L. Rodon, G. Folch, M. A. Carmona, R. M. Prieto-Sanchez, I. Barba, E. Martinez-Saez, L. Prudkin, I. Cuartas, C. Raventos, F. Martinez-Ricarte, M. A. Poca, D. Garcia-Dorado, M. M. Lahn, J. M. Yingling, J. Rodon, J. Sahuquillo, J. Baselga and J. Seoane (2010). "TGF-beta Receptor Inhibitors Target the CD44(high)/Id1(high) Glioma-Initiating Cell Population in Human Glioblastoma." Cancer Cell **18**(6): 655-668.

Azzam, E. I., J.-P. Jay-Gerin and D. Pain (2012). "Ionizing radiation-induced metabolic oxidative stress and prolonged cell injury." Cancer letters **327**(0): 48-60.

Bao, S., Q. Wu, R. E. McLendon, Y. Hao, Q. Shi, A. B. Hjelmeland, M. W. Dewhirst, D. D. Bigner and J. N. Rich (2006). "Glioma stem cells promote radioresistance by preferential activation of the DNA damage response." Nature **444**(7120): 756-760.

Berezovsky, A. D., L. M. Poisson, D. Cherba, C. P. Webb, A. D. Transou, N. W. Lemke, X. Hong, L. A. Hasselbach, S. M. Irtenkauf, T. Mikkelsen and A. C. deCarvalho (2014). "Sox2 promotes malignancy in glioblastoma by regulating plasticity and astrocytic differentiation." Neoplasia **16**(3): 193-206, 206 e119-125.

Bexell, D., S. Gunnarsson, P. Siesjo, J. Bengzon and A. Darabi (2009). "CD133+ and nestin+ tumor-initiating cells dominate in N29 and N32 experimental gliomas." Int J Cancer **125**(1): 15-22.

Bonnet, D. and J. E. Dick (1997). "Human acute myeloid leukemia is organized as a hierarchy that originates from a primitive hematopoietic cell." Nat Med **3**(7): 730-737.

Brat, D. J., A. A. Castellano-Sanchez, S. B. Hunter, M. Pecot, C. Cohen, E. H. Hammond, S. N. Devi, B. Kaur and E. G. Van Meir (2004). "Pseudopalisades in Glioblastoma Are Hypoxic, Express Extracellular Matrix Proteases, and Are Formed by an Actively Migrating Cell Population." Cancer Research **64**(3): 920.

Bush, N. A. O., S. M. Chang and M. S. Berger (2017). "Current and future strategies for treatment of glioma." Neurosurgical Review **40**(1): 1-14.

Campos, B., F.-S. Centner, J. L. Bermejo, R. Ali, K. Dorsch, F. Wan, J. Felsberg, R. Ahmadi, N. Grabe, G. Reifenberger, A. Unterberg, J. Burhenne and C. Herold-Mende (2011). "Aberrant Expression of Retinoic Acid Signaling Molecules Influences Patient Survival in Astrocytic Gliomas." The American Journal of Pathology **178**(5): 1953-1964.

Carruthers, R., S. U. Ahmed, K. Strathdee, N. Gomez-Roman, E. Amoah-Buahin, C. Watts and A. J. Chalmers (2015). "Abrogation of radioresistance in glioblastoma stem-like cells by inhibition of ATM kinase." Molecular Oncology **9**(1): 192-203.

Chacko, A. M., C. Li, D. A. Pryma, S. Brem, G. Coukos and V. Muzykantov (2013). "Targeted delivery of antibody-based therapeutic and imaging agents to CNS tumors: crossing the blood-brain barrier divide." Expert Opin Drug Deliv **10**(7): 907-926.

Chang, L., P. Graham, J. Hao, J. Ni, J. Deng, J. Bucci, D. Malouf, D. Gillatt and Y. Li (2016). "Cancer stem cells and signaling pathways in radioresistance." Oncotarget **7**(10): 11002-11017.

Chang, L., D. A. N. Zhao, H.-B. Liu, Q.-S. Wang, P. Zhang, C.-L. Li, W.-Z. Du, H.-J. Wang, X. Liu, Z.-R. Zhang and C.-L. Jiang (2015). "Activation of sonic hedgehog signaling enhances cell migration and invasion by induction of matrix metalloproteinase-2 and -9 via the phosphoinositide-3 kinase/AKT signaling pathway in glioblastoma." Molecular Medicine Reports **12**(5): 6702-6710.

Chen, Y.-C., Y.-W. Chen, H.-S. Hsu, L.-M. Tseng, P.-I. Huang, K.-H. Lu, D.-T. Chen, L.-K. Tai, M.-C. Yung, S.-C. Chang, H.-H. Ku, S.-H. Chiou and W.-L. Lo (2009). "Aldehyde dehydrogenase 1 is a putative marker for cancer stem cells in head and neck squamous cancer." Biochemical and Biophysical Research Communications **385**(3): 307-313.

Cojoc, M., C. Peitzsch, I. Kurth, F. Trautmann, L. A. Kunz-Schughart, G. D. Telegeev, E. A. Stakhovsky, J. R. Walker, K. Simin, S. Lyle, S. Fuessel, K. Erdmann, M. P. Wirth, M. Krause, M. Baumann and A. Dubrovska (2015). "Aldehyde Dehydrogenase Is Regulated by beta-Catenin/TCF and Promotes Radioresistance in Prostate Cancer Progenitor Cells." Cancer Res **75**(7): 1482-1494.

Combs, S. E., S. Rieken, W. Wick, A. Abdollahi, A. von Deimling, J. Debus and C. Hartmann (2011). "Prognostic significance of IDH-1 and MGMT in patients with glioblastoma: one step forward, and one step back?" Radiat Oncol **6**: 115.

Croker, A. K., M. Rodriguez-Torres, Y. Xia, S. Pardhan, H. S. Leong, J. D. Lewis and A. L. Allan (2017). "Differential Functional Roles of ALDH1A1 and ALDH1A3 in Mediating Metastatic Behavior and Therapy Resistance of Human Breast Cancer Cells." Int J Mol Sci **18**(10).

Cuddapah, V. A., S. Robel, S. Watkins and H. Sontheimer (2014). "A neurocentric perspective on glioma invasion." Nature reviews. Neuroscience **15**(7): 455-465.

Dahan, P., J. Martinez Gala, C. Delmas, S. Monferran, L. Malric, D. Zentkowski, V. Lubrano, C. Toulas, E. Cohen-Jonathan Moyal and A. Lemarie (2014). "Ionizing radiations sustain glioblastoma cell dedifferentiation to a stem-like phenotype through survivin: possible involvement in radioresistance." Cell Death & Disease **5**(11): e1543.

Dick, J. E. (2009). "Looking ahead in cancer stem cell research." Nat Biotech **27**(1): 44-46.

Diehn, M., R. W. Cho, N. A. Lobo, T. Kalisky, M. J. Dorie, A. N. Kulp, D. Qian, J. S. Lam, L. E. Ailles, M. Wong, B. Joshua, M. J. Kaplan, I. Wapnir, F. M. Dirbas, G. Somlo, C. Garberoglio, B. Paz, J. Shen, S. K. Lau, S. R. Quake, J. M. Brown, I. L. Weissman and M. F. Clarke (2009). "Association of reactive oxygen species levels and radioresistance in cancer stem cells." Nature **458**(7239): 780-783.

Diserens, A. C., N. de Tribolet, A. Martin-Achard, A. C. Gaide, J. F. Schnegg and S. Carrel (1981). "Characterization of an established human malignant glioma cell line: LN-18." Acta Neuropathologica **53**(1): 21-28.

Duester, G. (2000). "Families of retinoid dehydrogenases regulating vitamin A function: production of visual pigment and retinoic acid." Eur J Biochem **267**(14): 4315-4324.

Filatova, A., T. Acker and B. K. Garvalov (2013). "The cancer stem cell niche(s): the crosstalk between glioma stem cells and their microenvironment." Biochim Biophys Acta **1830**(2): 2496-2508.

Furnari, F. B., T. Fenton, R. M. Bachoo, A. Mukasa, J. M. Stommel, A. Stegh, W. C. Hahn, K. L. Ligon, D. N. Louis, C. Brennan, L. Chin, R. A. DePinho and W. K. Cavenee (2007). "Malignant astrocytic glioma: genetics, biology, and paths to treatment." Genes Dev **21**(21): 2683-2710.

Galli, R., E. Binda, U. Orfanelli, B. Cipelletti, A. Gritti, S. De Vitis, R. Fiocco, C. Foroni, F. Dimeco and A. Vescovi (2004). "Isolation and characterization of tumorigenic, stem-like neural precursors from human glioblastoma." Cancer Res **64**(19): 7011-7021.

Ginestier, C., M. H. Hur, E. Charafe-Jauffret, F. Monville, J. Dutcher, M. Brown, J. Jacquemier, P. Viens, C. G. Kleer, S. Liu, A. Schott, D. Hayes, D. Birnbaum, M. S. Wicha and G. Dontu (2007). "ALDH1 is a marker of normal and malignant human mammary stem cells and a predictor of poor clinical outcome." Cell Stem Cell **1**(5): 555-567.

Hart, M. G., R. Garside, G. Rogers, M. Somerville, K. Stein and R. Grant (2011). "Chemotherapy wafers for high grade glioma." Cochrane Database of Systematic Reviews(3).

Heddleston, J. M., Z. Li, R. E. McLendon, A. B. Hjelmeland and J. N. Rich (2009). "The hypoxic microenvironment maintains glioblastoma stem cells and promotes reprogramming towards a cancer stem cell phenotype." Cell Cycle **8**(20): 3274-3284.

Hegi, M. E., A. C. Diserens, T. Gorlia, M. F. Hamou, N. de Tribolet and M. Weller (2005). "MGMT gene silencing and benefit from temozolomide in glioblastoma." N Engl J Med **352**.

Hess, D. A., L. Wirthlin, T. P. Craft, P. E. Herrbrich, S. A. Hohm, R. Lahey, W. C. Eades, M. H. Creer and J. A. Nolta (2006). "Selection based on CD133 and high aldehyde dehydrogenase activity isolates long-term reconstituting human hematopoietic stem cells." Blood **107**(5): 2162.

Hou, L. C., A. Veeravagu, A. R. Hsu and V. C. K. Tse (2006). "Recurrent glioblastoma multiforme: a review of natural history and management options." Neurosurgical Focus **20**(4): E3.

Hundsberger, T., A. F. Hottinger, U. Roelcke, P. Roth, D. Migliorini, P. Y. Dietrich, K. Conen, G. Pesce, E. Hermann, A. Pica, M. W. Gross, D. Brügge, L. Plasswilm, M. Weller and P. M. Putora (2016). "Patterns of care in recurrent glioblastoma in Switzerland: a multicentre national approach based on diagnostic nodes." Journal of Neuro-Oncology **126**(1): 175-183.

IARC (International Agency for Research on Cancer), W. h. o. (2014). "World Cancer Report 2014."

Inukai, M., A. Hara, Y. Yasui, T. Kumabe, T. Matsumoto and M. Saegusa (2015). "Hypoxia-mediated cancer stem cells in pseudopalisades with activation of hypoxia-inducible factor-1alpha/Akt axis in glioblastoma." Hum Pathol **46**(10): 1496-1505.

Jiang, F., Q. Qiu, A. Khanna, N. W. Todd, J. Deepak, L. Xing, H. Wang, Z. Liu, Y. Su, S. A. Stass and R. L. Katz (2009). "Aldehyde Dehydrogenase 1 Is a Tumor Stem Cell-Associated Marker in Lung Cancer." Molecular cancer research : MCR **7**(3): 330-338.

Jin, X., X. Jin, J.-E. Jung, S. Beck and H. Kim (2013). "Cell surface Nestin is a biomarker for glioma stem cells." Biochemical and Biophysical Research Communications **433**(4): 496-501.

Kahlert, C., F. Bergmann, J. Beck, T. Welsch, C. Mogler, E. Herpel, S. Dutta, T. Niemietz, M. Koch and J. Weitz (2011). "Low expression of aldehyde deyhdrogenase 1A1 (ALDH1A1) is a prognostic marker for poor survival in pancreatic cancer." BMC Cancer **11**: 275-275.

Karsy, M., J. Guan, R. Jensen, L. E. Huang and H. Colman (2016). "The Impact of Hypoxia and Mesenchymal Transition on Glioblastoma Pathogenesis and Cancer Stem Cells Regulation." World Neurosurgery **88**: 222-236.

Keime-Guibert, F., O. Chinot, L. Taillandier, S. Cartalat-Carel, M. Frenay, G. Kantor, J.-S. Guillamo, E. Jadaud, P. Colin, P.-Y. Bondiau, P. Meneï, H. Loiseau, V. Bernier, J. Honnorat, M. Barrié, K. Mokhtari, J.-J. Mazeron, A. Bissery and J.-Y. Delattre (2007). "Radiotherapy for Glioblastoma in the Elderly." New England Journal of Medicine **356**(15): 1527-1535.

Kelley, K., J. Knisely, M. Symons and R. Ruggieri (2016). "Radioresistance of Brain Tumors." Cancers **8**(4): 42.

Khasraw, M., M. S. Ameratunga, R. Grant, H. Wheeler and N. Pavlakis (2014). "Antiangiogenic therapy for high-grade glioma." Cochrane Database of Systematic Reviews(9).

Kong, D. and V. Kotraiah (2012). "Modulation of Aldehyde Dehydrogenase Activity Affects (±)-4-Hydroxy-2E-nonenal (HNE) Toxicity and HNE–Protein Adduct Levels in PC12 Cells." Journal of Molecular Neuroscience **47**(3): 595-603.

Koppaka, V., D. C. Thompson, Y. Chen, M. Ellermann, K. C. Nicolaou, R. O. Juvonen, D. Petersen, R. A. Deitrich, T. D. Hurley and V. Vasiliou (2012). "Aldehyde Dehydrogenase Inhibitors: a Comprehensive Review of the Pharmacology, Mechanism of Action, Substrate Specificity, and Clinical Application." Pharmacological Reviews **64**(3): 520.

Kreso, A. and John E. Dick (2014). "Evolution of the Cancer Stem Cell Model." Cell Stem Cell **14**(3): 275-291.

Lämmer, F. (2016). Impact of aldehyde Dehydrogenase isotypes on xenograft and syngeneic mouse models of human primary glioblastoma multiforme, LMU München.

Lassen, N., J. B. Bateman, T. Estey, J. R. Kuszak, D. W. Nees, J. Piatigorsky, G. Duester, B. J. Day, J. Huang, L. M. Hines and V. Vasiliou (2007). "Multiple and Additive Functions of ALDH3A1 and ALDH1A1: CATARACT PHENOTYPE AND OCULAR OXIDATIVE DAMAGE IN Aldh3a1(–/–)/Aldh1a1(–/–) KNOCK-OUT MICE." The Journal of biological chemistry **282**(35): 25668-25676.

Lawrence, Y. R., M. V. Mishra, M. Werner-Wasik, D. W. Andrews, T. N. Showalter, J. Glass, X. Shen, Z. Symon and A. P. Dicker (2012). "Improving prognosis of glioblastoma in the 21st century: Who has benefited most?" Cancer **118**(17): 4228-4234.

Leinung, M., B. Ernst, C. DÖRing, J. Wagenblast, A. Tahtali, M. Diensthuber, T. StÖVer and C. Geissler (2015). "Expression of ALDH1A1 and CD44 in primary head and neck squamous cell carcinoma and their value for carcinogenesis, tumor progression and cancer stem cell identification." Oncology Letters **10**(4): 2289-2294.

Li, C., D. G. Heidt, P. Dalerba, C. F. Burant, L. Zhang, V. Adsay, M. Wicha, M. F. Clarke and D. M. Simeone (2007). "Identification of Pancreatic Cancer Stem Cells." Cancer Research **67**(3): 1030.

Li, T., Y. Su, Y. Mei, Q. Leng, B. Leng, Z. Liu, S. A. Stass and F. Jiang (2009). "ALDH1A1 is a marker for malignant prostate stem cells and predictor of prostate cancer patients' outcome." Lab Invest **90**(2): 234-244.

Li, T., Y. Su, Y. Mei, Q. Leng, B. Leng, Z. Liu, S. A. Stass and F. Jiang (2010). "ALDH1A1 is a marker for malignant prostate stem cells and predictor of prostate cancer patients' outcome." Lab Invest **90**(2): 234-244.

Liu, Y., D.-l. Lv, J.-j. Duan, S.-l. Xu, J.-f. Zhang, X.-j. Yang, X. Zhang, Y.-h. Cui, X.-w. Bian and S.-c. Yu (2014). "ALDH1A1 expression correlates with clinicopathologic features and poor prognosis of breast cancer patients: a systematic review and meta-analysis." BMC Cancer **14**: 444-444.

Loeffler, J., E. Alexander, III, F. H. Hochberg, P. Y. Wen, J. H. Morris, W. C. Schoene, R. L. Siddon, R. H. Morse and P. M. Black (1990). "Clinical patterns of failure following stereotactic interstitial irradiation for malignant gliomas." International Journal of Radiation Oncology • Biology • Physics **19**(6): 1455-1462.

Lun, M., E. Lok, S. Gautam, E. Wu and E. T. Wong (2011). "The natural history of extracranial metastasis from glioblastoma multiforme." Journal of Neuro-Oncology **105**(2): 261-273.

Maher, E. A., F. B. Furnari, R. M. Bachoo, D. H. Rowitch, D. N. Louis, W. K. Cavenee and R. A. DePinho (2001). "Malignant glioma: genetics and biology of a grave matter." Genes Dev **15**(11): 1311-1333.

Marchitti, S. A., C. Brocker, D. Stagos and V. Vasiliou (2008). "Non-P450 aldehyde oxidizing enzymes: the aldehyde dehydrogenase superfamily." Expert opinion on drug metabolism & toxicology **4**(6): 697-720.

Meng, E., A. Mitra, K. Tripathi, M. A. Finan, J. Scalici, S. McClellan, L. M. da Silva, E. Reed, L. A. Shevde, K. Palle and R. P. Rocconi (2014). "ALDH1A1 Maintains Ovarian Cancer Stem Cell-Like Properties by Altered Regulation of Cell Cycle Checkpoint and DNA Repair Network Signaling." PLoS ONE **9**(9): e107142.

Meng, J., P. Li, Q. Zhang, Z. Yang and S. Fu (2014). "A radiosensitivity gene signature in predicting glioma prognostic via EMT pathway." Oncotarget **5**(13): 4683-4693.

Mihatsch, J., M. Toulany, P. M. Bareiss, S. Grimm, C. Lengerke, R. Kehlbach and H. P. Rodemann (2011). "Selection of radioresistant tumor cells and presence of ALDH1 activity in vitro." Radiotherapy and Oncology **99**(3): 300-306.

Moreb, J. S., D. A. Ucar-Bilyeu and A. Khan (2017). "Use of retinoic acid/aldehyde dehydrogenase pathway as potential targeted therapy against cancer stem cells." Cancer Chemother Pharmacol **79**(2): 295-301.

Munthe, S., M. D. Sorensen, M. Thomassen, M. Burton, T. A. Kruse, J. D. Lathia, F. R. Poulsen and B. W. Kristensen (2016). "Migrating glioma cells express stem cell markers and give rise to new tumors upon xenografting." J Neurooncol **130**(1): 53-62.

Komission Leitlinie der Deutschen Gesellschaft für Neurologie (2012 (with addendum 2014)). "S2k Leitlinien für Diagnostik und Therapie in der Neurologie; Gliome, Aufl. 5"

Niederreither, K., V. Fraulob, J. M. Garnier, P. Chambon and P. Dolle (2002). "Differential expression of retinoic acid-synthesizing (RALDH) enzymes during fetal development and organ differentiation in the mouse." Mech Dev **110**(1-2): 165-171.

Ohgaki, H., P. Dessen, B. Jourde, S. Horstmann, T. Nishikawa, P. L. Di Patre, C. Burkhard, D. Schuler, N. M. Probst-Hensch, P. C. Maiorka, N. Baeza, P. Pisani, Y. Yonekawa, M. G. Yasargil, U. M. Lutolf and P. Kleihues (2004). "Genetic pathways to glioblastoma: a population-based study." Cancer Res **64**(19): 6892-6899.

Ohgaki, H. and P. Kleihues (2005). "Population-based studies on incidence, survival rates, and genetic alterations in astrocytic and oligodendroglial gliomas." J Neuropathol Exp Neurol **64**(6): 479-489.

Ohgaki, H. and P. Kleihues (2013). "The Definition of Primary and Secondary Glioblastoma." Clinical Cancer Research **19**(4): 764.

Oria, V. O., P. Bronsert, A. R. Thomsen, M. C. Foll, C. Zamboglou, L. Hannibal, S. Behringer, M. L. Biniossek, C. Schreiber, A. L. Grosu, L. Bolm, D. Rades, T. Keck, M. Werner, U. F. Wellner and O. Schilling (2018). "Proteome Profiling of Primary Pancreatic Ductal Adenocarcinomas Undergoing Additive Chemoradiation Link ALDH1A1 to Early Local Recurrence and Chemoradiation Resistance." Transl Oncol **11**(6): 1307-1322.

Ostrom, Q. T., L. Bauchet, F. G. Davis, I. Deltour, J. L. Fisher, C. E. Langer, M. Pekmezci, J. A. Schwartzbaum, M. C. Turner, K. M. Walsh, M. R. Wrensch and J. S. Barnholtz-Sloan (2014). "The epidemiology of glioma in adults: a "state of the science" review." Neuro Oncol **16**(7): 896-913.

Ramirez, Y. P., J. L. Weatherbee, R. T. Wheelhouse and A. H. Ross (2013). "Glioblastoma multiforme therapy and mechanisms of resistance." Pharmaceuticals (Basel) **6**(12): 1475-1506.

Rasper, M., A. Schafer, G. Piontek, J. Teufel, G. Brockhoff, F. Ringel, S. Heindl, C. Zimmer and J. Schlegel (2010). "Aldehyde dehydrogenase 1 positive glioblastoma cells show brain tumor stem cell capacity." Neuro Oncol **12**(10): 1024-1033.

Rees, J., R. Bradford, S. Brandner, N. Fersht, R. Jäger and E. Wilson (2016). Neuro-Oncology. Neurology, John Wiley & Sons, Ltd**:** 849-904.

Rieken, S., D. Habermehl, A. Mohr, L. Wuerth, K. Lindel, K. Weber, J. Debus and S. E. Combs (2011). "Targeting α(v)β(3)and α(v)β(5)inhibits photon-induced hypermigration of malignant glioma cells." Radiation Oncology (London, England) **6**: 132-132.

Ropolo, M., A. Daga, F. Griffero, M. Foresta, G. Casartelli, A. Zunino, A. Poggi, E. Cappelli, G. Zona, R. Spaziante, G. Corte and G. Frosina (2009). "Comparative Analysis of DNA Repair in Stem and Nonstem Glioma Cell Cultures." Molecular Cancer Research **7**(3): 383.

Sarkaria, J. N., G. J. Kitange, C. D. James, R. Plummer, H. Calvert, M. Weller and W. Wick (2008). "Mechanisms of Chemoresistance in Malignant Glioma." Clinical cancer research : an official journal of the American Association for Cancer Research **14**(10): 2900-2908.

Schäfer, A. (2012). Aldehyde dehydrogenase 1 A1 is expressed by cancer stem cells and mediates chemoresistance in human glioblastoma, Technical university Munich.

Schäfer, A., J. Teufel, F. Ringel, M. Bettstetter, I. Hoepner, M. Rasper, J. Gempt, J. Koeritzer, F. Schmidt-Graf, B. Meyer, C. P. Beier and J. Schlegel (2012). "Aldehyde dehydrogenase 1A1—a new mediator of resistance to temozolomide in glioblastoma." Neuro-Oncology **14**(12): 1452-1464.

Schwartzbaum, J. A., J. L. Fisher, K. D. Aldape and M. Wrensch (2006). "Epidemiology and molecular pathology of glioma." Nat Clin Pract Neuro **2**(9): 494-503.

Scott, J., Y.-Y. Tsai, P. Chinnaiyan and H.-H. M. Yu (2011). "Effectiveness of Radiotherapy for Elderly Patients With Glioblastoma." International Journal of Radiation Oncology*Biology*Physics **81**(1): 206-210.

Shankar, A., S. Kumar, A. S. Iskander, N. R. Varma, B. Janic, A. deCarvalho, T. Mikkelsen, J. A. Frank, M. M. Ali, R. A. Knight, S. Brown and A. S. Arbab (2014). "Subcurative radiation significantly increases cell proliferation, invasion, and migration of primary glioblastoma multiforme in vivo." Chin J Cancer **33**(3): 148-158.

Shi, X., Y. Zhang, J. Zheng and J. Pan (2012). "Reactive oxygen species in cancer stem cells." Antioxid Redox Signal **16**(11): 1215-1228.

Singh, S. K., C. Hawkins, I. D. Clarke, J. A. Squire, J. Bayani, T. Hide, R. M. Henkelman, M. D. Cusimano and P. B. Dirks (2004). "Identification of human brain tumour initiating cells." Nature **432**(7015): 396-401.

Sladek, N. E. (2003). "Human aldehyde dehydrogenases: potential pathological, pharmacological, and toxicological impact." J Biochem Mol Toxicol **17**(1): 7-23.

Soehngen, E., A. Schaefer, J. Koeritzer, V. Huelsmeyer, C. Zimmer, F. Ringel, J. Gempt and J. Schlegel (2014). "Hypoxia upregulates aldehyde dehydrogenase isoform 1 (ALDH1) expression and

induces functional stem cell characteristics in human glioblastoma cells." Brain Tumor Pathology **31**(4): 247-256.

Sottoriva, A., I. Spiteri, S. G. Piccirillo, A. Touloumis, V. P. Collins, J. C. Marioni, C. Curtis, C. Watts and S. Tavare (2013). "Intratumor heterogeneity in human glioblastoma reflects cancer evolutionary dynamics." Proc Natl Acad Sci U S A **110**(10): 4009-4014.

Stupp, R., M. E. Hegi, W. P. Mason, M. J. van den Bent, M. J. Taphoorn, R. C. Janzer, S. K. Ludwin, A. Allgeier, B. Fisher, K. Belanger, P. Hau, A. A. Brandes, J. Gijtenbeek, C. Marosi, C. J. Vecht, K. Mokhtari, P. Wesseling, S. Villa, E. Eisenhauer, T. Gorlia, M. Weller, D. Lacombe, J. G. Cairncross, R. O. Mirimanoff, R. European Organisation for, T. Treatment of Cancer Brain, G. Radiation Oncology and G. National Cancer Institute of Canada Clinical Trials (2009). "Effects of radiotherapy with concomitant and adjuvant temozolomide versus radiotherapy alone on survival in glioblastoma in a randomised phase III study: 5-year analysis of the EORTC-NCIC trial." Lancet Oncol **10**(5): 459-466.

Stupp, R., W. P. Mason, M. J. van den Bent, M. Weller, B. Fisher, M. J. B. Taphoorn, K. Belanger, A. A. Brandes, C. Marosi, U. Bogdahn, J. Curschmann, R. C. Janzer, S. K. Ludwin, T. Gorlia, A. Allgeier, D. Lacombe, J. G. Cairncross, E. Eisenhauer and R. O. Mirimanoff (2005). "Radiotherapy plus Concomitant and Adjuvant Temozolomide for Glioblastoma." New England Journal of Medicine **352**(10): 987-996.

Sundar, S. J., J. K. Hsieh, S. Manjila, J. D. Lathia and A. Sloan (2014). "The role of cancer stem cells in glioblastoma." Neurosurg Focus **37**(6): E6.

Tanaka, K., H. Tomita, K. Hisamatsu, T. Nakashima, Y. Hatano, Y. Sasaki, S. Osada, T. Tanaka, T. Miyazaki, K. Yoshida and A. Hara (2015). "ALDH1A1-overexpressing cells are differentiated cells but not cancer stem or progenitor cells in human hepatocellular carcinoma." Oncotarget **6**(28): 24722-24732.

Vasiliou, V. and D. W. Nebert (2005). "Analysis and update of the human aldehyde dehydrogenase (ALDH) gene family." Human Genomics **2**(2): 138-143.

Verhaak, R. G. W., K. A. Hoadley, E. Purdom, V. Wang, Y. Qi, M. D. Wilkerson, C. R. Miller, L. Ding, T. Golub, J. P. Mesirov, G. Alexe, M. Lawrence, M. O'Kelly, P. Tamayo, B. A. Weir, S. Gabrie, W. Winckler, S. Gupta, L. Jakkula, H. S. Feiler, J. G. Hodgson, C. D. James, J. N. Sarkaria, C. Brennan, A. Kahn, P. T. Spellman, R. K. Wilson, T. P. Speed, J. W. Gray, M. Meyerson, G. Getz, C. M. Perou, D. N. Hayes and N. The Cancer Genome Atlas Research (2010). "An integrated genomic analysis identifies clinically relevant subtypes of glioblastoma characterized by abnormalities in PDGFRA, IDH1, EGFR and NF1." Cancer cell **17**(1): 98.

Wang, K., X. Chen, Y. Zhan, W. Jiang, X. Liu, X. Wang and B. Wu (2013). "Increased expression of ALDH1A1 protein is associated with poor prognosis in clear cell renal cell carcinoma." Med Oncol **30**(2): 574.

Wild-Bode, C., M. Weller, A. Rimner, J. Dichgans and W. Wick (2001). "Sublethal Irradiation Promotes Migration and Invasiveness of Glioma Cells." Cancer Research **61**(6): 2744.

Wilson, T. A., M. A. Karajannis and D. H. Harter (2014). "Glioblastoma multiforme: State of the art and future therapeutics." Surgical Neurology International **5**: 64.

Xiao, T., M. Shoeb, M. S. Siddiqui, M. Zhang, K. V. Ramana, S. K. Srivastava, V. Vasiliou and N. H. Ansari (2009). "Molecular Cloning and Oxidative Modification of Human Lens ALDH1A1: Implication in Impaired Detoxification of Lipid Aldehydes." Journal of Toxicology and Environmental Health, Part A **72**(9): 577-584.

Xu, S.-L., S. Liu, W. Cui, Y. Shi, Q. Liu, J.-J. Duan, S.-C. Yu, X. Zhang, Y.-H. Cui, H.-F. Kung and X.-W. Bian (2015). "Aldehyde dehydrogenase 1A1 circumscribes high invasive glioma cells and predicts poor prognosis." American Journal of Cancer Research **5**(4): 1471-1483.

Xu, X., S. Chai, P. Wang, C. Zhang, Y. Yang, Y. Yang and K. Wang (2015). "Aldehyde dehydrogenases and cancer stem cells." Cancer Letters **369**(1): 50-57.

Yan, Z., L. Xu, J. Zhang, Q. Lu, S. Luo and L. Xu (2016). "Aldehyde dehydrogenase 1A1 stabilizes transcription factor Gli2 and enhances the activity of Hedgehog signaling in hepatocellular cancer." Biochem Biophys Res Commun **471**(4): 466-473.

Yang, L., Y. Ren, X. Yu, F. Qian, B. S. Bian, H. L. Xiao, W. G. Wang, S. L. Xu, J. Yang, W. Cui, Q. Liu, Z. Wang, W. Guo, G. Xiong, K. Yang, C. Qian, X. Zhang, P. Zhang, Y. H. Cui and X. W. Bian (2014). "ALDH1A1 defines invasive cancer stem-like cells and predicts poor prognosis in patients with esophageal squamous cell carcinoma." Mod Pathol **27**(5): 775-783.

Zhai, G. G., R. Malhotra, M. Delaney, D. Latham, U. Nestler, M. Zhang, N. Mukherjee, Q. Song, P. Robe and A. Chakravarti (2006). "Radiation Enhances the Invasive Potential of Primary Glioblastoma Cells via Activation of the Rho Signaling Pathway." Journal of Neuro-Oncology **76**(3): 227-237.

Zong, H., R. G. Verhaak and P. Canoll (2012). "The cellular origin for malignant glioma and prospects for clinical advancements." Expert Rev Mol Diagn **12**(4): 383-394.